VIBRATION TRANSMISSION THROUGH

ROLLING ELEMENT BEARINGS

by

Serap OĞUZ

B.S. in M.E., Boğaziçi University, 1993

Submitted to the Institute for Graduate Studies in

Science and Engineering in partial fulfillment of

the requirements for the degree of

Master of Science

in

Mechanical Engineering

Boğaziçi University

1995

ACKNOWLEDGEMENTS

I would like to express my sincere gratitude to my thesis supervisors Assoc. Prof. Ahmet N. Ceranoğlu for his endless interest, guidance and encouragement throughout this study and Assoc. Prof. Osman S. Türkay for his helps in the experimental parts.

I would like to thank my father Mech. Eng., M.S., İlhami Oğuz for his support, helps in design and quick manufacturing of the experimental setup.

I would also like to thank my friends for their helps all along my study.

ABSTRACT

Current bearing models, based on either ideal boundary condition or purely translational stiffness element description, can not explain how the vibratory motion may be transmitted from the rotating shaft to the casing and other connecting structures of rotating machinery. Such simple models may be used to analyze the free and forced vibration of the rotor dynamic systems enclosed in rigid casings; however, these models lack the explanation of how the vibratory motion is transmitted from the rotating shaft to the flexible or rigid casing and other connecting structures. These models can only predict in plane type of motions of the flexible casing which is actually out of plane or flexural in nature. This paradox is essentially due to the incomplete understanding of bearing as a vibratory motion transmitter in rotating mechanical equipment.

In this work a mathematical model described by Lim and Singh for the precision rolling element bearings is applied to a rotor-bearing system.This model proposes a bearing stiffness matrix which demonstrates the coupling between the shaft bending motion and the motion of the casing or pedestals. Verification of this model is made experimentally using a simple rotor-bearing system which differs from the example cases of Lim and Singh. Acceleration of the pedestals are measured by piezoelectric accelerometers and compared with the theoretical results. Theoretical force and moment transmissibilities of the bearing and mount is calculated. Making the vibration analysis in this manner allows us to calculate the bearing moment transmissibility which can not be calculated by simple models.

ÖZET

Rulmanı ideal sınır şartları ya da doğrusal yay elemanı olarak kabul eden modeller titreşim hareketinin dönen milden şaseye ve diğer birimlere nasıl aktarıldığını tam olarak ifade edemezler. Bu basit modeller rijit şase üzerindeki dinamik rotor sistemlerinin serbest ve zorlanmış titreşim analizlerinde kullanılabilir, ancak dönen milden esnek ya da rijit şaseye veya diğer birimlere titreşim iletimini hesaplamakta yetersiz kalırlar. Gerçekte düzlem dışı olan esnek şase üzerindeki hareketleri düzlemsel kabul ederler ki, bu da rulmanın titreşim hareketinin iletilmesindeki etkisinin yetersiz anlaşılmasından kaynaklanır.

Bu çalışmada Lim ve Singh'in rulmanlar için oluşturdukları yeni bir matematiksel model, bir rotor rulman sistemine uygulandı. Rulmanın yaylanmasını, milin eğilme hareketiyle şasenin hareketini birbirine bağlayan bir matrisle ifade eden bu model, bilyalı rulmanların kullanıldığı, Lim ve Singh'in verdikleri örmeklerden bazı açılardan farklı, basit bir rotor-rulman sistemi kullanılarak deneysel olarak desteklendi. Yatakların ivmeleri, piezoelektrik accelerometreyle ölçülüp, teorik sonuçlarla karşılaştırıldı. Teorik olarak rulmanın kuvvet ve moment iletiminin milin dönüş hızına göre değişimi hesaplandı. Bu şekilde yapılan titreşim analizi, basit modellerce bulunamayan, rulman moment iletimini de hesaplama imkanı oluşturdu.

TABLE OF CONTENTS

LIST OF FIGURES

LIST OF TABLES

LIST OF SYMBOLS

A_0	Unloaded distance between the inner and outer raceway groove curvature centers
A_j	Loaded distance between the inner and outer raceway groove curvature centers
a_0 , a_i	Locations of outer and inner raceway groove curvature centers
[C]	System damping matrix
d_{bi}	Inner raceway diameter of bearing
d_{bm}	Bearing pitch diameter
d_{bo}	Outer raceway diameter of bearing
E_C	Rayleigh dissipation function
E_T	Kinetic energy
E_U	Potential energy
EI	Flexural rigidity of the shaft
$F_{jba}(t)$	Alternating bearing force in the j=x,y,z direction
$F_{jbm}(t)$	Mean bearing force in the j=x,y,z direction
$F_{ja}(t)$	Applied alternating force on the shaft in the j=x,y,z direction
$F_{jm}(t)$	Applied mean force on the shaft in the j=x,y,z direction
F_w	Generalized force in Lagrangian formulation
$\{f(t)\}_a$	Generalized alternating applied load vector
$\{f\}_{bm}$	Mean bearing load vector
$\{f\}_{sm}$	Mean shaft load vector
G	Shear modulus of elasticity
H_k	Nonlinear functions defined in Newton-Raphson method explanation, k=1,2,3,..5
I_{jc}	Mass moment of inertia of the casing about j=x, y or z axis
I_{jp}	Mass moment of inertia of the pedestal about j=x, y or z axis
{I}	Lumped inertia row vector

K_n	Rolling element load-deflection stiffness constant
[K]	System stiffness matrix
$[K]_{bm}$	Bearing stiffness matrix of dimension six
$[K]_s$	Shaft stiffness matrix
$[K]_s^e$	Shaft segment stiffness matrix
$[K]_v$	Mount stiffness matrix
k_{vj}	Mount stiffness coefficient, j=x, y, z, q_x,q_y, q_z
k_{bwj}	Bearing stiffness coefficient, w,j=x, y, z, q_x, q_y, q_z
L_e	Shaft segment length
[M]	System mass matrix
$M_{j\,ba}$	Alternating bearing moment vector about j=x or y direction
$M_{j\,bm}$	Mean bearing moment vector about j=x or y direction
m_R	Rotor mass
m_s	Shaft mass
m_{sej}	Shaft lumped mass
m_c	Casing mass
m_p	Pedestal mass
{m}	Lumped mass row vector
n	Rolling element load-defşlection exponent
n_s	Number of shaft segments
Q_j	Resultant normal load on the jth rolling element
$\{q(t)\}_a$	Generalized alternating displacement vector
$\{q\}_{bm}$	Mean bearing displacement vector
$\{q(t)\}_{ca}$	Alternating casing displacement vector
$\{q(t)\}_{pa}$	Alternating pedestal displacement vector
$\{q(t)\}_{sa}$	Alternating shaft displacement vector
$\{q(t)\}_{sm}$	Mean shaft displacement vector
$\{q\}_w$	Generalized displacement vector in Lagrangian formulation
R_j	jth bearing coordinate vector, j=1,n_s ,n_s+1
[R]	Rotation matrix in Jacobi method
$[R]_k$	Rotation matrix for the kth iteration step in Jacobi method

1. INTRODUCTION

1.1 ASPECTS OF ROTOR BEARING SYSTEM

The study of rotor dynamics has in recent years become of increasing importance in the engineering design of systems. With the increase in performance requirements of high speed rotating machinery in various fields, the problem of designing a unit capable of smooth operation under various conditions of speed and load is faced. Since a large class of rotating machinery operates near or above their first critical speed, it is necessary to study flexible rotor dynamics.

Current models in rotor dynamics accept precision rolling element bearings either as ideal boundary conditions for the shafts or as purely translational stiffness elements. Such simple bearing models may be adequate for the free and forced vibration analyses of the rotor dynamic system enclosed in a rigid casing but these mathematical models cannot predict the vibration transmissibility between the rotating shaft and flexible or rigid casing.

A schematic of a generic system with a flexible shaft rotating at speed Ω_z and subjected to a mean load vector $\{f\}_{sm}=\{F_{im}, T_{im}\}$, i=x,y,z , with flexible casing and mount is shown in Figure 1.1 ; the shaft is supported by ball bearings. In the new model, Lim and Singh [1] propose a bearing stiffness matrix $[K]_{bm}$ which is expected to demonstrate the coupling between the shaft bending motion and the flexural motion of the casing. The translational bearing stiffness coefficients currently used in rotor dynamics are only a small subset of the proposed bearing stiffness matrix $[K]_{bm}$.

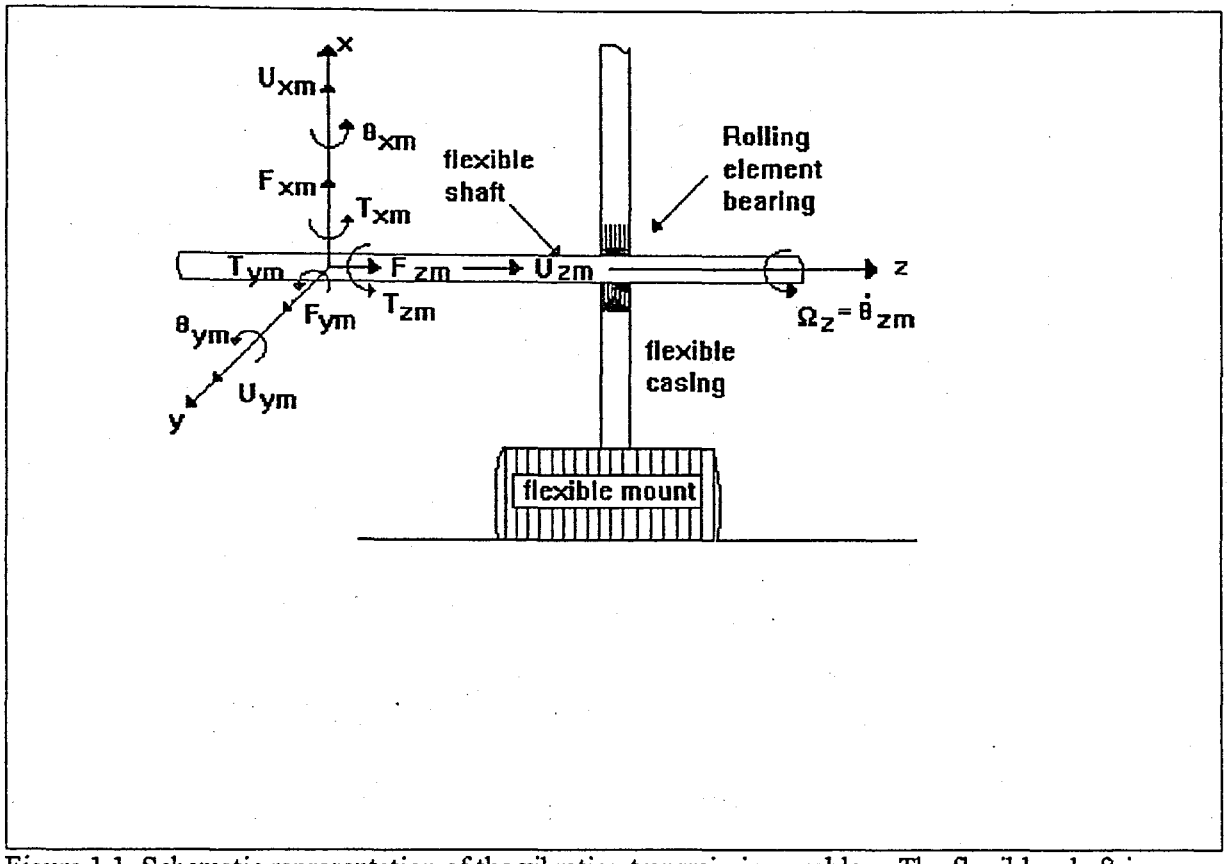

Figure 1.1 Schematic representation of the vibration transmission problem. The flexible shaft is subjected to mean forces F_{im} and torques T_{im}, where i=x,y,z is the direction and subscript m implies mean. Also, θ is the angular displacement and u is the translational displacement.

1.2 GENERAL BACKGROUND

The ideal boundary conditions for the shaft have been assumed to be simply supported for short bearings, clamped for long bearings and free (in the torsional mode only) [2]. In all other cases, bearing is described as time-invariant translational springs with stiffness coefficients k_{brr} and/or k_{bzz} in the radial and axial directions, respectively [3]. Harris [4] and Garguilo [5] have given formulas for such non-linear stiffness coefficients. These are derived from the radial or axial mean force-displacement equations. Their derivations neglect the effects of radial clearance and mean bearing force vector $\{f\}_{bm}$ on the load distribution and hence are applicable only for a constant load angle Ψ_l of 180 degrees (Fig. 2.1). White [6] refined these formulations by using a finite difference approximation for the computation of stiffness

coefficients for radial ball and roller bearings, and by including the effects of radial clearance and force on the load angle Ψ_l. Even with these refinements the mathematical model is still inadequate and incapable of predicting the vibration transmission across bearings due to the incompleteness of the bearing stiffness matrix..

In 1982 Rajab as stated by Limand Singh[1], realized the limitations of these simple theories and philosophically proposed two additional stiffness terms $k_{br\theta}$ and $k_{b\theta\theta}$ which couple the relative radial and rotational bearing displacements between the inner and outer rings, given the mean radial load and moment about the axis transverse to the radial line of action. In 1988 Young as stated by Lim and Singh[1], while still retaining other features of Rajab's model, extended his analysis to include the mean axial force F_{bzm}. Using a discrete summation over all of the loaded rolling elements, he obtained the bearing forces and moments instead of using integral form.

Experimental determination of the bearing stiffness coefficients has been strictly limited to the translational coefficients k_{brr} and k_{bzz}. A method for the measurement of an *in situ* bearing stiffness under oscillating loading conditions was given by Walford and Stone[7]. Recently Kraus [8] designed an in situ measurement test stand to determine the translational bearing stiffness from measured vibration spectra, in conjunction with the single-degree-of-freedom-system theory. They determine the effect of preload, bearing release and rotational speed Ω_Z on k_{brr} and k_{bzz}. Their results show that k_{brr} and k_{bzz} are essentially linear, and that the effect of Ω_Z is negligible when a high preload is applied on the bearing.

In 1990 Lim and Singh [1] developed a new mathematical model to analyze vibration transmission properties of the bearing by considering a bearing stiffness matrix of dimension six that clearly demonstrates a coupling between the shaft bending motion and the flexural motion of the casing plate.

1.3 OBJECT OF THE STUDY AND PRESENTATION OF THE WORK

The specific objectives of this study are as follows: (i)by using the bearing stiffness matrix proposed by Lim and Singh [1] to develop the bearing stiffness matrix $[K]_{bm}$ for new example cases to analyze the vibration transmission through bearings; (ii) to develop a numerical scheme to compute bearing stiffness matrix $[K]_{bm}$ and discuss the existence of solutions of the non-linear algebraic bearing equations describing load-displacement relationships; (iii) to incorporate the proposed bearing matrix $[K]_{bm}$, in the linear discrete vibration model of the rotating mechanical equipment; (iv) to find eigen solutions and forced harmonic responses, and predict vibration transmission through ball bearings; (v) to validate the theory developed by Lim and Singh [1,9,10] by comparing theoretical and experimental results of an analogous system. Finally it should be noted that dimensionless parameters will not be used here as metric units are invariably employed to specify bearings.

The cases considered in this study differ from the ones used by Lim and Singh [9]; we have used two different kinds of ball bearings, angular contact, deep groove types of, and two rotors introducing two additional degrees of freedom.

2. BEARING STIFFNESS FORMULATION

2. 1 ASSUMPTIONS

The formulation of bearing stiffness matrix proposed by Lim and Singh [1], $[K]_{bm}$ for ball bearings is based on the following assumptions: (i) ball bearings have elliptical contacts between the inner race, rolling elements and outer race when loaded, and (ii) the loaded contact angles α_j of ball bearings shown in Fig. 2.2, may change as opposed to roller bearings. Each bearing is characterized by its kinematic and design parameters such as unloaded contact angle α_0, radial clearance r_L, effective stiffness coefficient K_n for inner ring-single rolling element-outer ring contacts, angular misalignment and radius of inner raceway groove curvature [9,11].

The mean bearing displacements $\{q\}_{bm}$ as shown in Figure 2.1 are given by the relative rigid body motions between the inner and outer rings. The total bearing displacement vector is given as $\{q\}_b = \{q\}_{bm} + \{q\}_{ba}(t)$, where $\{q\}_{ba}(t)$ is the fluctuation about the mean point $\{q\}_{bm}$ during the steady state rotation. Accordingly, one must consider time varying bearing stiffness coefficients. However in our analysis, such time varying bearing stiffness coefficients are neglected by assuming very small vibratory motions, i.e., $\{q\}_{ba} << \{q\}_{bm}$, and high bearing preloads. Consequently, only the mean bearing loads and displacements are included in the derivation of $[K]_{bm}$. the basic load-deflection relation for each elastic rolling element is defined by the Hertzian contact stress theory [9], and the load experienced by each rolling element is described by its relative location in the bearing raceway. Further it is assumed that the angular position of each rolling element relative to one another is always maintained due to the rigid cages and pin retainers. Secondary effects such as centrifugal forces and gyroscopic moments on the bearing are ignored as these effects are evident only at extremely high rotational speeds. Tribological issues are beyond the scope of this study and hence in our analysis the bearings are assumed to be unlubricated.

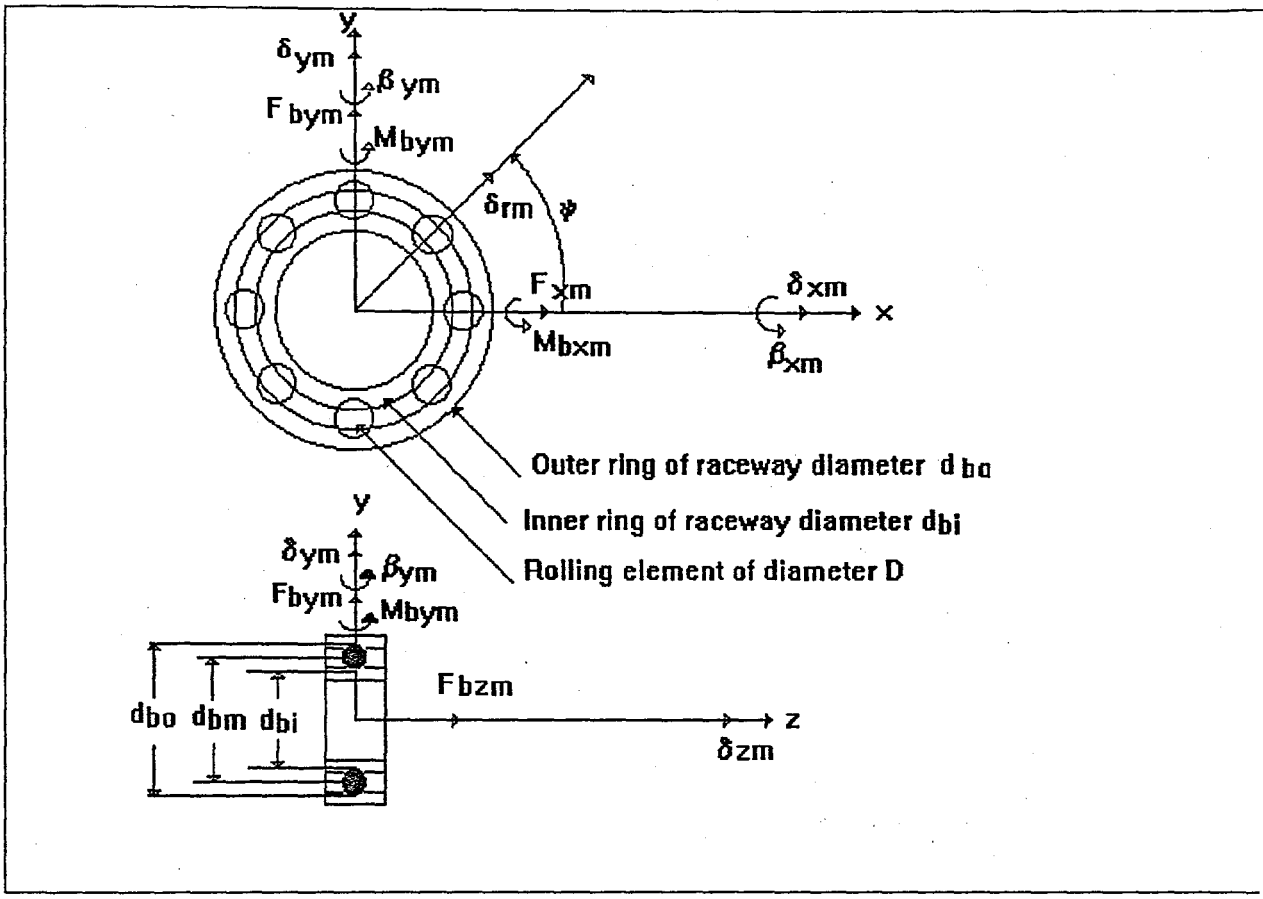

Figure 2.1 Rolling element bearing kinematics and co-ordinate system. d_{bo} is the outer raceway diameter, d_{bm} is the bearing pitch diameter, d_{bi} is the inner raceway diameter, y is the angular position of rolling element, d_{im} is the mean translational disolacement, b_{pm} is the mean angular displacement, F_{bim} is the mean bearing force, and M_{bpm} is the mean bearing moment where i=x,y,z and p=x,y are the directions.

2. 2 BEARING LOAD-DISPLACEMENT RELATIONS

The mean applied loads $\{ f \}_{sm}$ on the shaft were given in figure 1.1. Bearing preloads give rise to the mean bearing displacements $\{q\}_{bm}$ and loads $\{f\}_{bm}$. These displacements $\{q\}_{bm}$ are used to derive the resultant elastic deformation $\delta(\psi_j)$ of the jth rolling element located at angle ψ_j from the x-axis .

$$\delta_B(\phi_j) = \begin{cases} A(\phi_j) - A_0 , & \delta_{Bj} \rangle 0 \\ 0, & \delta_{Bj} \langle 0 \end{cases} \qquad (2.1\ a)$$

$$A (\psi_j) = [(\delta^*)^2_{zj} + (\delta^*)^2_{rj}]^{1/2} \qquad (2.1\ b)$$

$$(\delta^*)_{zj} = A_0 \sin \alpha_0 + (\delta)_{zj} \qquad (2.1\ c)$$

$$(\delta^*)_{rj} = A_0 \cos \alpha_0 + (\delta)_{rj} \qquad (2.1\ d)$$

where A_0 and A_j are the unloaded and loaded relative distances between the inner (a_i) and outer (a_o) raceway groove curvature centers respectively. The ratio of ball radius to track radius is called osculation. In Equation (2.1) the effective jth rolling element displacements in the axial $(\delta)_{zj}$ and radial $(\delta)_{rj}$ directions are shown in Figure 2.2 in terms of the bearing displacements $\{q\}_{bm}$:

$$(\delta)_{zj} = \delta_z + r_j \{ \beta_{xm} \sin(\psi_j) - \beta_{ym} \cos(\psi_j) \} \qquad (2.2\ a)$$

$$(\delta)_{rj} = \delta_{xm} \cos(\psi_j) + \delta_{ym} \sin(\psi_j) - r_L \qquad (2.2\ b)$$

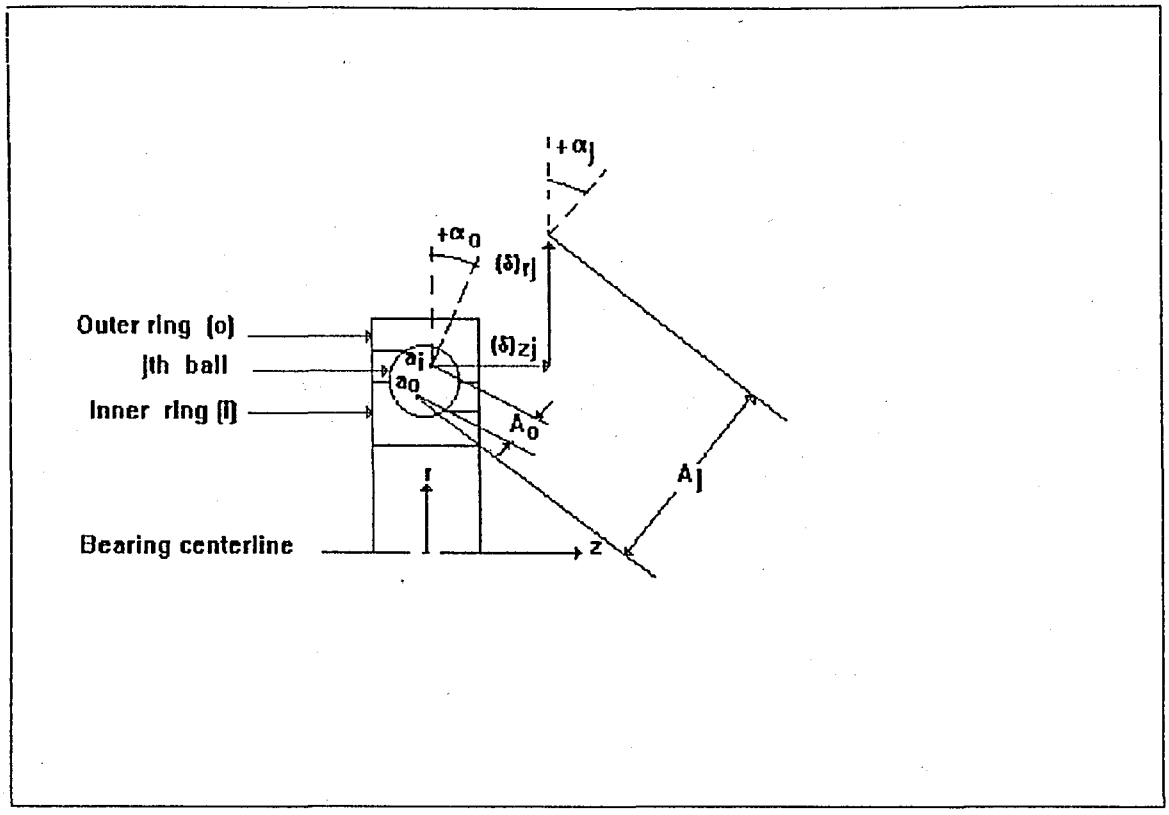

Fig 2. 2 Elastic deformation of rolling element for non-constant contact angle α_j given by the change in the distance between the inner a_i and outer a_o raceway groove radius curvature centers due to the mean bearing loads or displacements

where r_j is the radial distance of the inner raceway groove curvature center for the ball bearing. equations (2.1) and (2.2) in conjunction with the Hertzian contact stress principle [9,11] yield the following load-deflection relationships for a single rolling element:

$$Q_j = K_n \delta_j^n \qquad (2.3)$$

where Q_j is the resultant normal load on the rolling element, and K_n is the effective stiffness constant for the inner race-rolling element-outer race contacts and is a function of the bearing geometry and material properties. The exponent n is 3/2 for ball bearings. The sign convention for α_j is positive when measured from the bearing x-y plane towards the axial z-axis as shown in Fig. 2.3. The loaded contact angle α_j is given by,

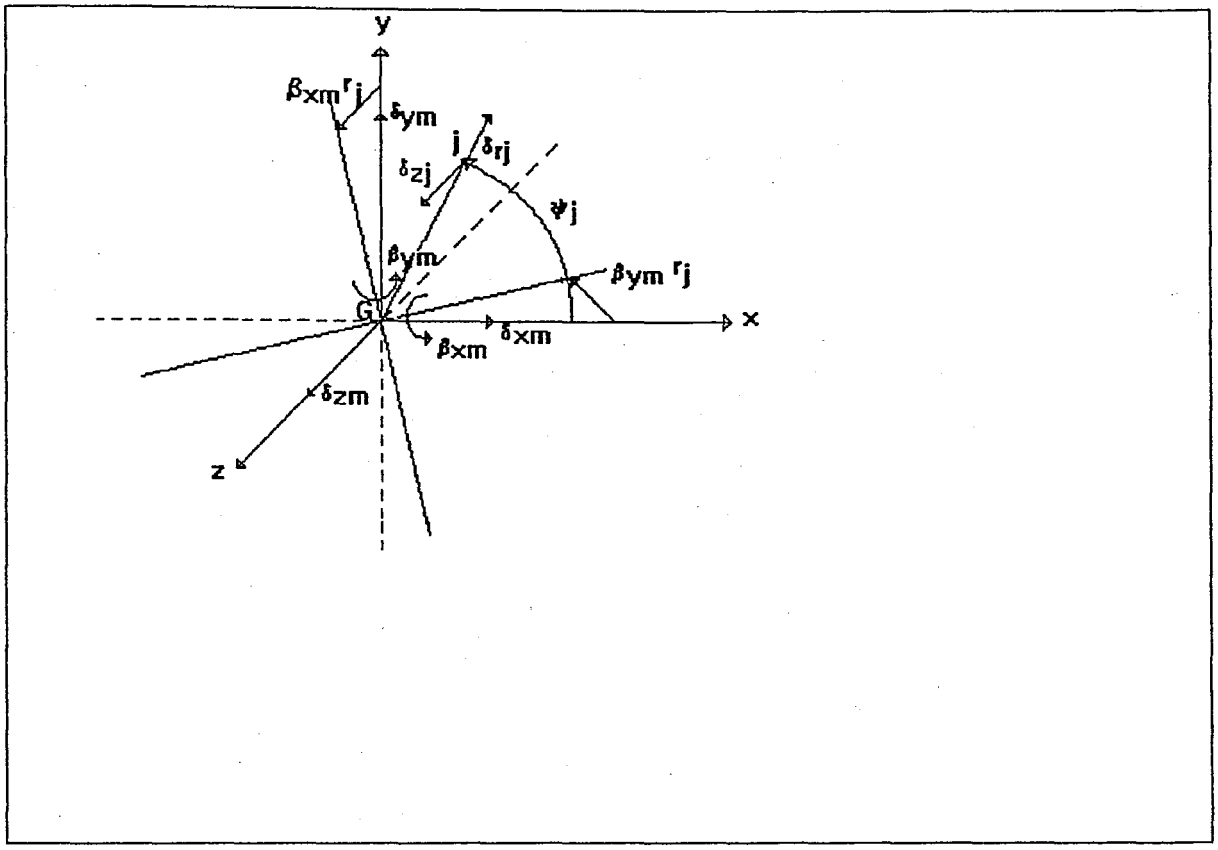

Figure 2.3 Decomposition of the effective radial $(\delta)_{rj}$ and axial $(\delta)_{zj}$ deformations of the jth rolling elementin terms of the mean bearing displacements $\{ q \}_{bm}$. Here G is the bearing outer ring geometrical center.

$$\tan (\alpha_j) = \{ A_0 \sin \alpha_0 + (\delta)_{zj} \} / \{ A_0 \cos \alpha_0 + (\delta)_{rj} \} \qquad (2.4)$$

2. 3 DEVELOPMENT OF BEARING STIFFNESS MATRIX

Bearing stiffness matrix $[K]_{bm}$ is a global representation of the bearing kinematic and elastic characteristics as it combines the effects of z number of loaded rolling element stiffness in parallel by $\delta_{Bj} > 0$. Resultant bearing mean load vector $\{f\}_{bm}$ is related to the bearing displacement vector $\{q\}_{bm}$ by Lim and Singh [1] through vectorial sums:

$$\begin{Bmatrix} Mbxm \\ Mbym \\ Mbzm \end{Bmatrix} \equiv \sum_{j}^{z} rj\, Qj \sin\alpha j \begin{Bmatrix} \sin\psi j \\ -\cos\psi j \\ 0 \end{Bmatrix} \qquad (2.5\ a)$$

$$\begin{Bmatrix} Fbxm \\ Fbym \\ Fbzm \end{Bmatrix} = \sum_{j}^{z} Qj \begin{Bmatrix} \cos\alpha j \cos\psi j \\ \cos\alpha j \sin\psi j \\ \sin\alpha j \end{Bmatrix} \qquad (2.5\ b)$$

Expressing Q_j and α_j in Equation (2.5) in terms of $\{\delta_{im}, \beta_{im}\}$ yields the following explicit relationships between $\{ f \}_{bm}$ and $\{ q \}_{bm}$ for ball bearings:

$$\begin{Bmatrix} M_{bxm} \\ M_{bym} \\ M_{bzm} \end{Bmatrix} = K_n \sum_{j}^{z} \frac{\left\{ \sqrt{\left[A_0 \sin\alpha_0 + (\delta)_{zj}\right]^2 + \left[A_0 \cos\alpha_0 + (\delta)_{rj}\right]^2} - A_0 \right\}^n}{\sqrt{\left[A_0 \sin\alpha_0 + (\delta)_{zj}\right]^2 + \left[A_0 \cos\alpha_0 + (\delta)_{rj}\right]^2}} * r_j \left\{ A_0 \sin\alpha_0 + (\delta)_{zj} \right\} \begin{Bmatrix} \sin\psi_j \\ -\cos\psi_j \\ 0 \end{Bmatrix} \qquad (2.6a)$$

$$\begin{Bmatrix} F_{bxm} \\ F_{bym} \\ F_{bzm} \end{Bmatrix} = K_n \sum_{j}^{z} \frac{\left\{ \sqrt{\left[A_0 \sin\alpha_0 + (\delta)_{zj}\right]^2 + \left[A_0 \cos\alpha_0 + (\delta)_{rj}\right]^2} - A_0 \right\}^n}{\sqrt{\left[A_0 \sin\alpha_0 + (\delta)_{zj}\right]^2 + \left[A_0 \cos\alpha_0 + (\delta)_{rj}\right]^2}} * \begin{Bmatrix} \left[A_0 \cos\alpha_0 + (\delta)_{rj}\right] \cos\psi_j \\ \left[A_0 \cos\alpha_0 + (\delta)_{rj}\right] \sin\psi_j \\ \left[A_0 \sin\alpha_0 + (\delta)_{zj}\right] \end{Bmatrix} \qquad (2.6b)$$

A symmetric bearing stiffness matrix [K]$_{bm}$ of dimension six is defined from Equations (2.5 a) and (2.5 b) and by assuming that { q }$_{ba}$<< { q }$_{bm}$:

$$[K]_{bm} = \begin{bmatrix} \frac{\partial F_{bim}}{\partial \delta_{jm}} & \frac{\partial F_{bim}}{\partial \beta_{jm}} \\ \frac{\partial M_{bim}}{\partial \delta_{jm}} & \frac{\partial M_{bim}}{\partial \beta_{jm}} \end{bmatrix}_{\{q\}_{bm}} \quad i,j = x,y,z. \tag{2.7}$$

where each stiffness coefficient must be evaluated at the mean point {q}$_{bm}$. Explicit expressions for the ball bearing stiffness are as follows:

$$k_{bxx} = K_n \sum_j^z \frac{(A_j - A_0)^n \cos^2 \psi_j \left\{ \frac{nA_j(\delta^*)^2_{rj}}{A_j - A_0} + A_j^2 - (\delta^*)^2_{rj} \right\}}{A_j^3} \tag{2.8 a}$$

$$k_{bxy} = K_n \sum_j^z \frac{(A_j - A_0)^n \sin \psi_j \cos \psi_j \left\{ \frac{nA_j(\delta^*)^2_{rj}}{A_j - A_0} + A_j^2 - (\delta^*)^2_{rj} \right\}}{A_j^3} \tag{2.8 b}$$

$$k_{bxz} = K_n \sum_j^z \frac{(A_j - A_0)^n (\delta^*)_{rj} (\delta^*)_{zj} \cos \psi_j \left\{ \frac{nA_j}{A_j - A_0} - 1 \right\}}{A_j^3} \tag{2.8 c}$$

$$k_{bx\theta x} = K_n \sum_j^z \frac{r_j (A_j - A_0)^n (\delta^*)_{rj} (\delta^*)_{zj} \sin \psi_j \cos \psi_j \left\{ \frac{nA_j}{A_j - A_0} - 1 \right\}}{A_j^3} \tag{2.8 d}$$

$$k_{bx\theta_y} = K_n \sum_j^z \frac{r_j (A_j - A_0)^n (\delta^*)_{rj} (\delta^*)_{zj} \cos^2 \psi_j \left\{ 1 - \frac{nA_j}{A_j - A_0} \right\}}{{A_j}^3} \qquad (2.8\text{ e})$$

$$k_{byy} = K_n \sum_j^z \frac{(A_j - A_0)^n \sin^2 \psi_j \left\{ \frac{nA_j (\delta^*)^2 rj}{A_j - A_0} + {A_j}^2 - (\delta^*)^2 rj \right\}}{{A_j}^3} \qquad (2.8\text{ f})$$

$$k_{byz} = K_n \sum_j^z \frac{(A_j - A_0)^n (\delta^*)_{rj} (\delta^*)_{zj} \sin \psi_j \left\{ \frac{nA_j}{A_j - A_0} - 1 \right\}}{{A_j}^3} \qquad (2.8\text{ g})$$

$$k_{by\theta_x} = K_n \sum_j^z \frac{r_j (A_j - A_0)^n (\delta^*)_{rj} (\delta^*)_{zj} \sin^2 \psi_j \left\{ \frac{nA_j}{A_j - A_0} - 1 \right\}}{{A_j}^3} \qquad (2.8\text{ h})$$

$$k_{by\theta_y} = K_n \sum_j^z \frac{r_j (A_j - A_0)^n (\delta^*)_{rj} (\delta^*)_{zj} \sin \psi_j \cos \psi_j \left\{ 1 - \frac{nA_j}{A_j - A_0} \right\}}{{A_j}^3} \qquad (2.8\text{ i})$$

$$k_{bzz} = K_n \sum_j^z \frac{(A_j - A_0)^n \left\{ \frac{nA_j (\delta^*)^2 zj}{A_j - A_0} + {A_j}^2 - (\delta^*)^2 zj \right\}}{{A_j}^3} \qquad (2.8\text{ j})$$

$$k_{bz\theta_x} = K_n \sum_j^z \frac{r_j (A_j - A_0)^n \sin\psi_j \left\{ \frac{nA_j (\delta^*)^2_{zj}}{A_j - A_0} + A_j{}^2 - (\delta^*)^2_{zj} \right\}}{A_j{}^3} \qquad (2.8\text{ k})$$

$$k_{bz\theta_y} = K_n \sum_j^z \frac{r_j (A_j - A_0)^n \cos\psi_j \left\{ (\delta^*)^2_{zj} - \frac{nA_j (\delta^*)^2_{zj}}{A_j - A_0} - A_j{}^2 \right\}}{A_j{}^3} \qquad (2.8\text{ l})$$

$$k_{b\theta x\theta_x} = K_n \sum_j^z \frac{r^2{}_j (A_j - A_0)^n \sin^2\psi_j \left\{ \frac{nA_j (\delta^*)^2_{zj}}{A_j - A_0} + A_j{}^2 - (\delta^*)^2_{zj} \right\}}{A_j{}^3} \qquad (2.8\text{ m})$$

$$k_{b\theta_x\theta_y} = K_n \sum_j^z \frac{r^2{}_j (A_j - A_0)^n \cos\psi_j \sin\psi_j \left\{ (\delta^*)^2_{zj} - \frac{nA_j (\delta^*)^2_{zj}}{A_j - A_0} - A_j{}^2 \right\}}{A_j{}^3} \qquad (2.8\text{ n})$$

$$k_{b\theta_y\theta_y} = K_n \sum_j^z \frac{r^2{}_j (A_j - A_0)^n \cos^2\psi_j \left\{ \frac{nA_j (\delta^*)^2_{zj}}{A_j - A_0} + A_j{}^2 - (\delta^*)^2_{zj} \right\}}{A_j{}^3} \qquad (2.8\text{ o})$$

$$k_{bi\theta_z} = k_{b\theta_i\theta_z} = 0, \qquad i = x, y, z \qquad (2.8\text{ p})$$

It should be noted that all stiffness terms associated with the torsional degree of freedom β_{zm} are zero due to the fact that an ideal bearing allows free rotation about the z-direction.

2. 4 NUMERICAL ESTIMATION OF [K]$_{bm}$

The coefficients k_{bij} can be computed by one of the following two methods: 1), direct computation using the given mean bearing displacement vector $\{q\}_{bm}$ by employing Equations (2.8 a-p); 2), solving numerically the non-linear algebraic equations given by Eqs. (2.6 a,b) to obtain $\{q\}_{bm}$ from $\{f\}_{bm}$, and then evaluating k_{bij} using method 1. Bearing mean load vector $\{f\}_{bm}$ may be function of the mean shaft loads, bearing preloads, shaft and casing compliances, depending on the configuration and flexibility of the rotataing mechanical system.

Newton-Raphson method was adopted in the case of method 2 for its good convergence characteristic. To implement this method, Equation (2.5) for each bearing is rearranged as

$$\begin{Bmatrix} H_1 \\ H_2 \end{Bmatrix} = \begin{Bmatrix} M_{bxm} \\ M_{bym} \end{Bmatrix} - \sum_j^z r_j Q_j \sin\alpha_j \begin{Bmatrix} \sin\psi_j \\ -\cos\psi_j \end{Bmatrix} = \begin{Bmatrix} 0 \\ 0 \end{Bmatrix} \qquad (2.9\text{ a})$$

$$\begin{Bmatrix} H_3 \\ H_4 \\ H_5 \end{Bmatrix} = \begin{Bmatrix} F_{bxm} \\ F_{bym} \\ F_{bzm} \end{Bmatrix} - \sum_j^z Q_j \sin\alpha_j \begin{Bmatrix} \cos\alpha_j \cos\psi_j \\ \cos\alpha_j \sin\psi_j \\ \sin\alpha_j \end{Bmatrix} = \begin{Bmatrix} 0 \\ 0 \\ 0 \end{Bmatrix}, \qquad (2.9\text{ b})$$

$$H_k(X+\delta X) \approx H_k(X) + \sum_j^V \frac{\partial H_k}{\partial X_j}\delta X_j, \qquad (2.10)$$

The solution for the incremental vector δX can be obtained by setting $H_k(X+\delta X)=0$ per Equations (2.9)and (2.10) which yields a set of algebraic equations. This vector δX is added to the previously computed vector X obtained by setting $H_k(X)=0$ for the next iteration until the convergence criterion, say that δX is within a specified tolerance, is reached. Related fortran program is given in App. 1.

2.5 PARAMETRIC STUDIES

The stiffness matrix $[K]_{bm}$ includes a coupling between casing flexural motion and shaft bending motion that is reflected by off-diagonal, $k_{bx\theta y}$, $k_{by\theta x}$, $k_{bz\theta x}$ and $k_{bz\theta y}$, and rotational diagonal, $k_{b\theta x\theta x}$ and $k_{b\theta y\theta y}$, stiffness coefficients; these are labeled as *'coupling coefficients* [1].

The coupling coefficients given a constant radial bearing displacement δ_{rm} (radial preload), are found to increase as α_0 increases and reach a maximum when $\alpha_0=90^o$. On the other hand, the radial translational stiffness coefficients in the x and y directions are found to decrease as α_0 increases. These observations imply that for deep groove ball type bearing ($\alpha_0\approx 0^o$) the radial stiffness coefficients k_{brr} are dominant, but for angular contact ball type bearing ($\alpha_0>0^o$) the coupling terms are more significant (Fig. 2.4).

In the case when the ball bearings are subjected to mean axial displacement (axial preload), the number of non-zero stiffness coefficients are less than those seen for the radial preload only. Over mid to high α_0 values, the coupling coefficients are found to be significant. The translational stiffness coefficients are relatively constant except for the axial stiffness which increases as α_0 increases (Fig. 2.5).

Results for the misalignment in ball bearings simulated by specifying a mean bearing angular displacement β_{ym} show that the dominant stiffness coefficients are the same as those seen for the radial preload case. In the case of ball bearings most of the stiffness coefficients remain constant for $0^o\leq\alpha_0\leq 90^o$ (Fig. 2.6).

These results are stated by Lim and Singh [1]. By using the design parameters of the bearings used in the experimental part of this work (which are given in Table 4.1), Fig. 2.4, Fig. 2.5 and Fig 2.6 are obtained. These Figures represent an agreement with the results of Lim and Singh [1] in shape.

From the detailed parametric studies, it is concluded that the nature of $[K]_{bm}$ is dictated by the bearing type, α_0 and preloads. The results of all possible forms of $[K]_{bm}$ are listed in Table 2.1 for ball bearings.

Table 2.1

Proposed ball bearing stiffness coefficients; j=x,y; i=x,y but i≠j

Mean bearing loads	Mean bearing displacement			Stiffness coefficients
	$\alpha_0 \approx 0^o$	$0^o < \alpha_0 < 90^0$	$\alpha_0 \approx 90^o$	
F_{jm}	δ_{jm}	-	-	$k_{xx}, k_{yy}, k_{zz}, k_{\theta x \theta x}, k_{\theta y \theta y}, k_{z \theta i}$
F_{zm}	δ_{zm}	δ_{zm}	-	$k_{xx}, k_{yy}, k_{zz}, k_{\theta x \theta x}, k_{\theta y \theta y}, k_{x \theta y}, k_{y \theta x}$
F_{zm}	-	-	δ_{zm}	$k_{xx}, k_{yy}, k_{zz}, k_{\theta x \theta x}, k_{\theta y \theta y}$
M_{jm}	β_{jm}	-	-	$k_{xx}, k_{yy}, k_{zz}, k_{\theta x \theta x}, k_{\theta y \theta y}, k_{iz}$
F_{zm}, M_{jm}	-	-	δ_{zm}, β_{jm}	$k_{xx}, k_{yy}, k_{zz}, k_{\theta x \theta x}, k_{\theta y \theta y}, k_{z \theta j}$
F_{xm}, F_{ym}	δ_{xm}, δ_{ym}	-	-	$k_{xx}, k_{yy}, k_{zz}, k_{\theta x \theta x}, k_{\theta y \theta y}, k_{xy}, k_{\theta x \theta y}, k_{z \theta x}, k_{z \theta y}$
F_{jm}, M_{jm}	δ_{jm}, β_{jm}	-	-	$k_{xx}, k_{yy}, k_{zz}, k_{\theta x \theta x}, k_{\theta y \theta y}, k_{x \theta x}, k_{y \theta y}, k_{jz}, k_{z \theta j}$
Mxm,Mym	δ_{jm}, β_{jm}	-	-	$k_{xx}, k_{yy}, k_{zz}, k_{\theta x \theta x}, k_{\theta y \theta y}, k_{xy}, k_{xz}, k_{yz}, k_{\theta x \theta y}$
F_{jm}, F_{zm}, M_{im}	$\delta_{jm}, \delta_{zm}, \beta$ im	$\delta_{jm}, \delta_{zm}, \beta_{im}$	$\delta_{jm}, \delta_{zm}, \beta_{im}$	$k_{xx}, k_{yy}, k_{zz}, k_{\theta x \theta x}, k_{\theta y \theta y}, k_{x \theta y}, k_{y \theta x}, k_{jz}, k_{z \theta j}$
F_{zm}, M_{xm}, M_{ym}	$\delta_{zm}, \beta_{xm}, \beta$ ym	$\delta_{zm}, \beta_{xm}, \beta_{ym}$	$\delta_{zm}, \beta_{xm}, \beta_{ym}$	$k_{xx}, k_{yy}, k_{zz}, k_{\theta x \theta x}, k_{\theta y \theta y}, k_{xy}, k_{\theta x \theta y}, k_{z \theta x}, k_{z \theta y}$
$\{f\}_m$	Combinati ons	of $\{q\}_m$		All non-zero except θ_z terms

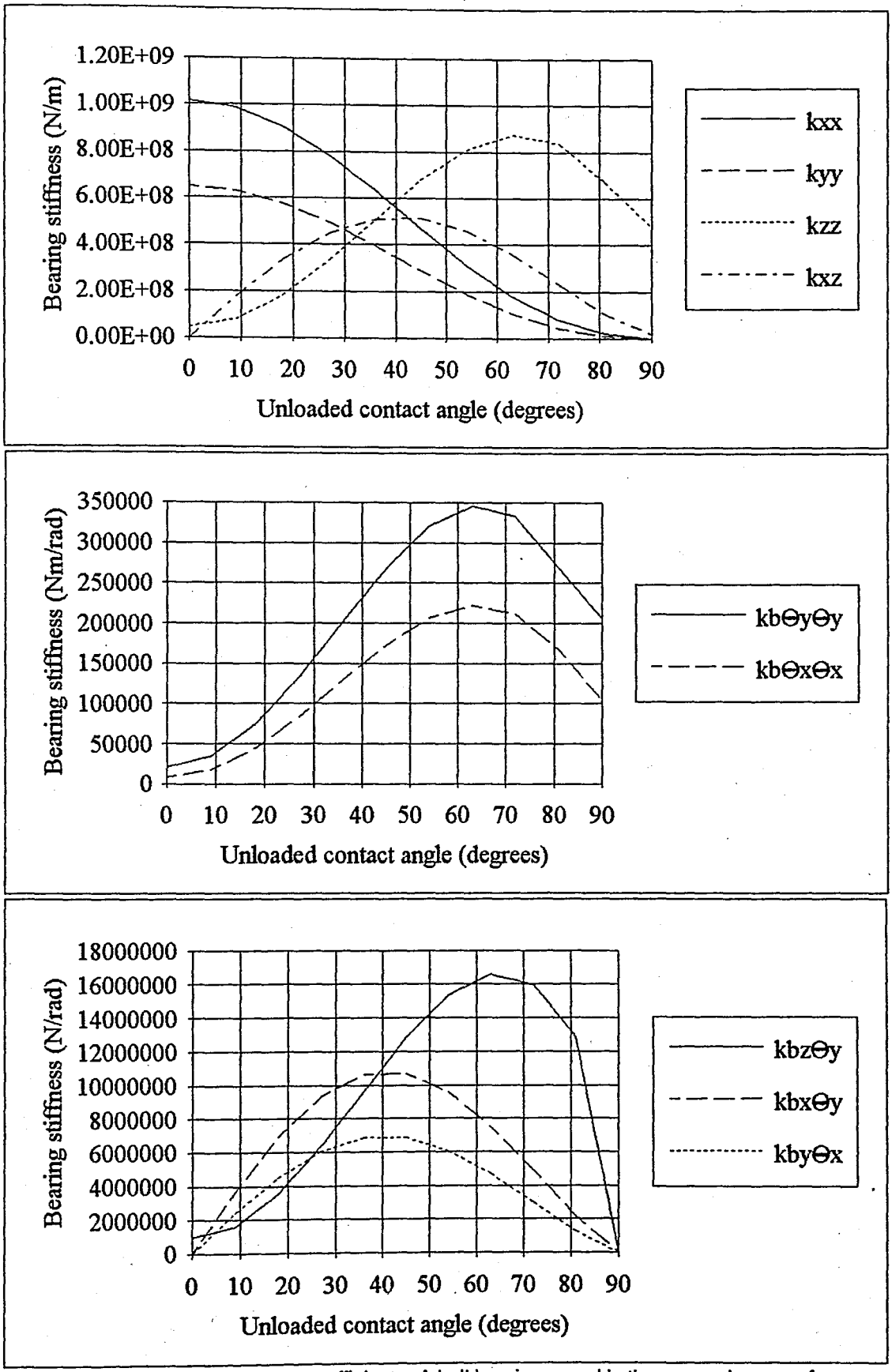

Fig. 2.4. Dominant stiffness coefficients of ball bearings used in the example cases for unloaded contact angle between 0 and 90 and given a constant mean radial displacement .025 mm in the x-direction.

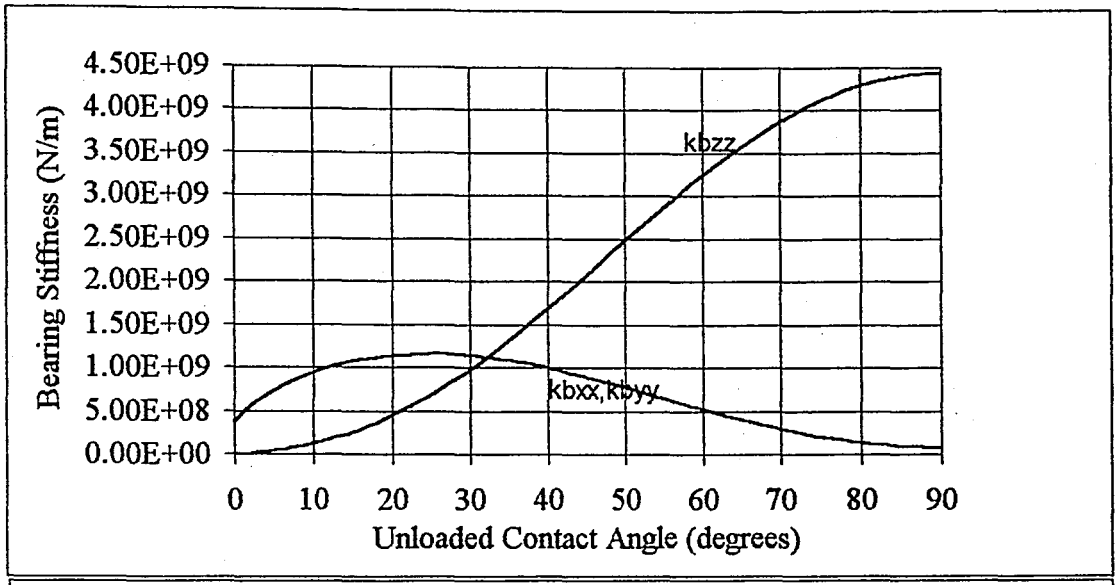

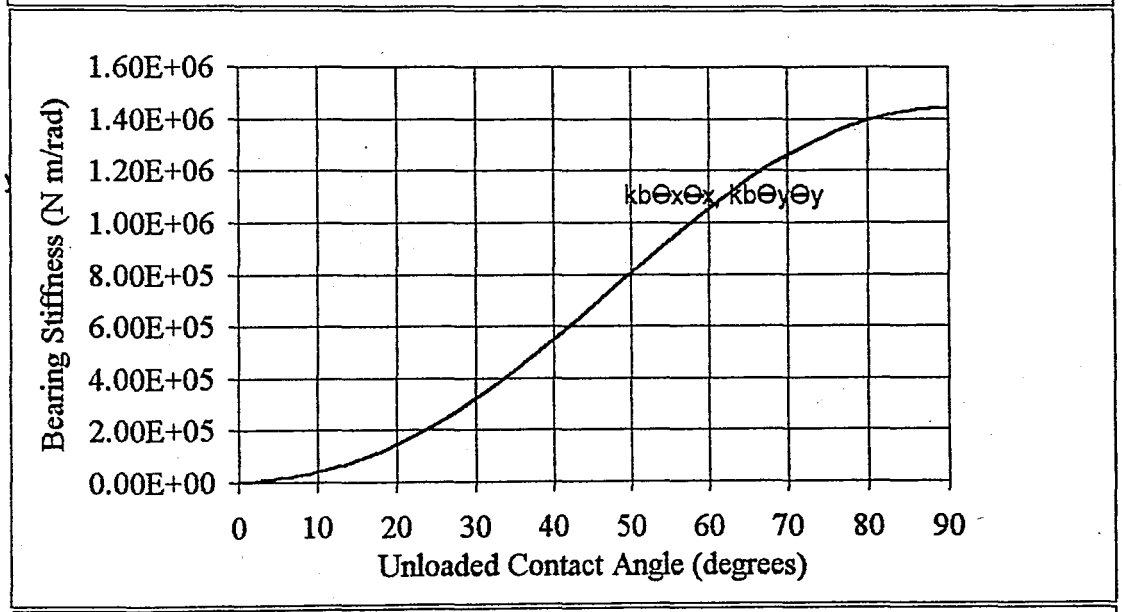

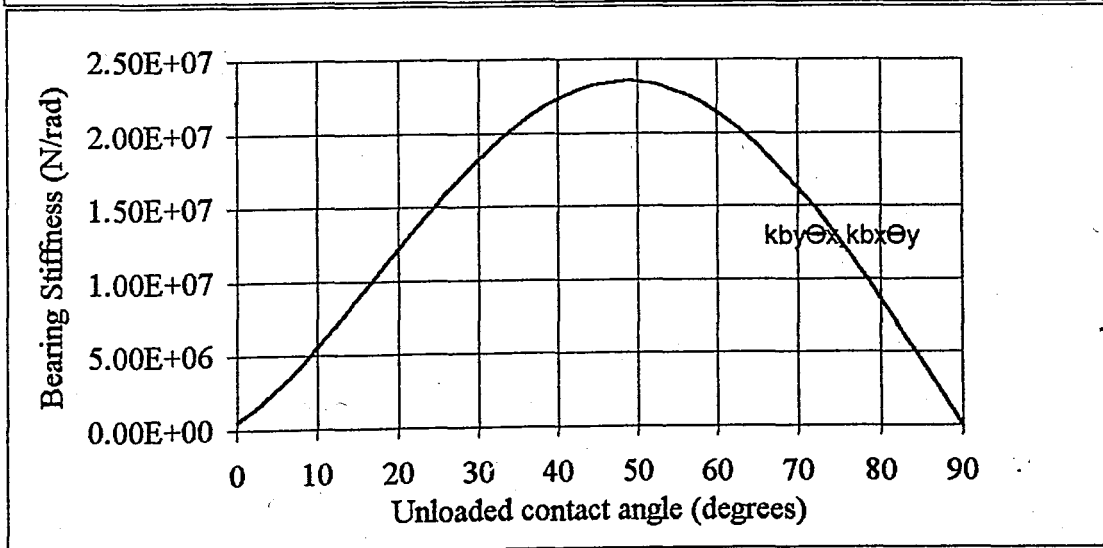

Fig. 2.5 Dominant stiffness coefficients of angular contact type of ball bearings used in the example cases for unloaded contact angle between 0 and 90 degrees and given a constant mean axial displacement .025 mm. (in the z-direction)

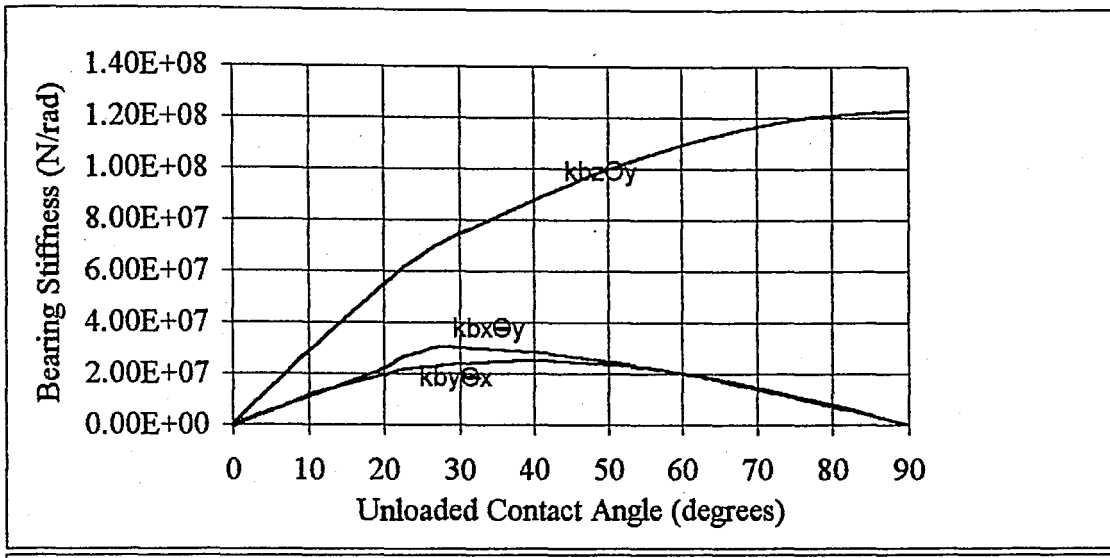

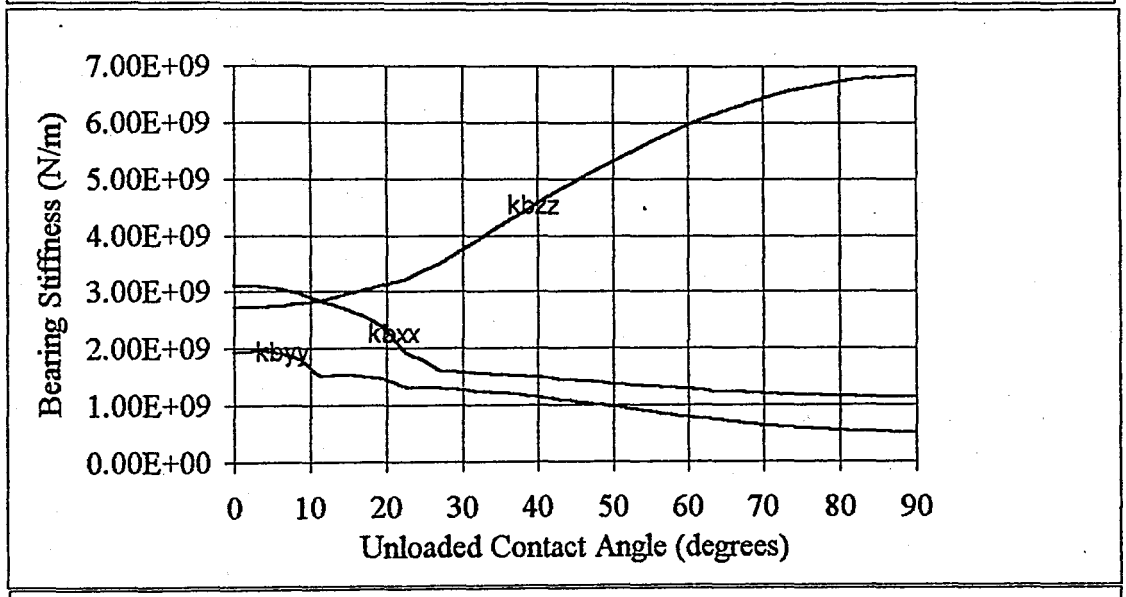

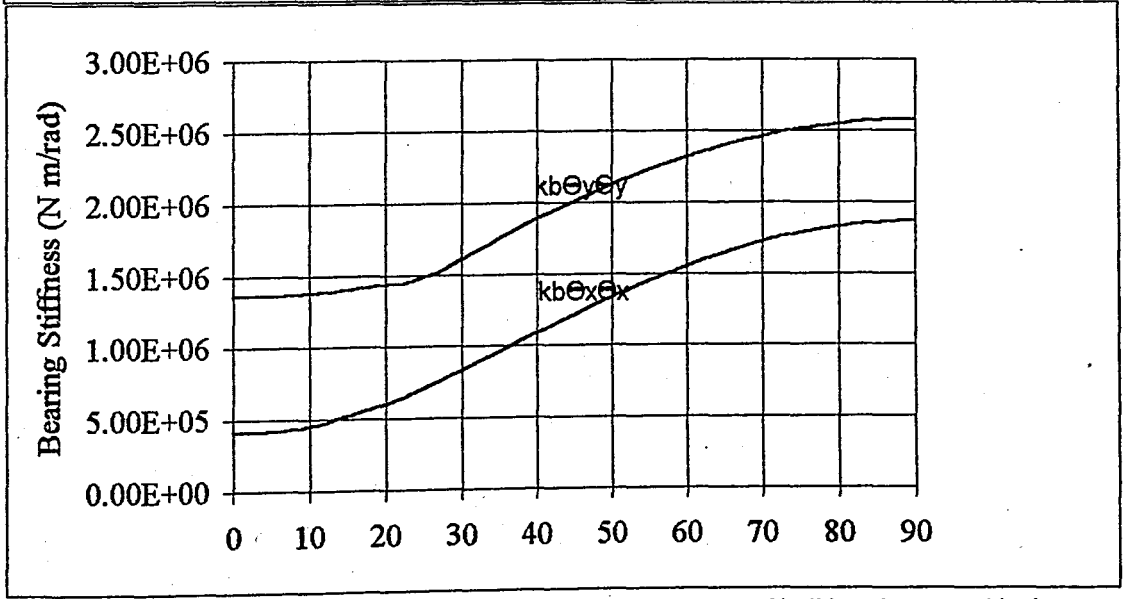

Fig. 2.6 Dominant stiffness coefficients of angular contact type of ball bearings used in the example cases for unloaded contact angle between 0 and 90 degrees and given a misalignment .015 rad. in the y-direction.

3. VIBRATION ANALYSIS OF THE SYSTEM

3.1 GOVERNING EQUATIONS

Linear lumped vibration model of the system shown in Fig.1.1 are used to incorporate $[K]_{bm}$ and to characterize the vibration transmission through rolling element bearings. The effect of gyroscopic moment on the shaft dynamics is not included. Since the bearing system is statically indeterminate, the direct stiffness formulation technique is used to obtain the system governing equations as opposed to the flexibility formulation. The governing equations for the vibration model is given in matrix form as,

$$[M]\left\{\ddot{q}(t)\right\}_a + [C]\left\{\dot{q}(t)\right\}_a + [K]\{q(t)\}_a = \{f(t)\}_a, \qquad (3.1)$$

where [M], [C] and [K] are the system mass, damping and stiffness matrices, respectively. Due to the linearity assumption of the vibrating system, mean shaft loads $\{f\}_{bm}$ and preloads do not directly affect the dynamic response of the rotating system and hence are excluded from Equation (3.1). However, $\{f\}_{bm}$ and bearing preloads are assumed to be constant to ensure a time-invariant $[K]_{bm}$ matrix which depends only on these mean loads or on the mean deflection operating points. Accordingly, only the alternating shaft loads $\{f(t)\}_{sa}$ in Fig.1.1 which represent typical machine excitation due to the kinematic errors, mass unbalances and torque fluctuations are included in the forced vibration problem. The energy dissipation associated with the rolling element bearings may be assumed to be an energy equivalent viscous damping matrix $[C]_b=\sigma[K]_{bm}$ where σ is the Rayleigh damping matrix proportionality constant. But damping is ignored in the following analysis.

The coupling coefficients of $[K]_{bm}$ provide the capability to predict casing rigid body angular $\theta_{jca}(t)$, j=x,y,z, and translational $u_{jca}(t)$ motions, given only the unidirectional transverse shaft forces. Hence the shaft motions can be coupled to the motions of the casing of a system. the bearing preloads can now be included in the mean shaft load vector $\{f\}_{bm}$ by a

direct vector addition, as the rigid shaft can be assumed to be a single lumped mass for this purpose. An alternating displacement vector $\{q(t)\}_a=\{\{q(t)\}_{sa}{}^T,\{q[t]\}_{ca}{}^T\}^T$, is defined, where $\{q(t)\}_{sa}=\{u_{jsa}(t)\ ,\ \theta_{jsa}(t)\}^T$ and $\{q(t)\}_{ca}=\{u_{jca}(t)\ ,\ \theta_{jca}(t)\}^T$, j=x,y,z, are the shaft and casing alternating displacement vectors respectively. The governing equations of motion for this generic vibration model with 12 degrees of freedom are given by Equation (3.1) with

$$[M]=\begin{bmatrix}[M]_s & [0]\\ [0] & [M]_c\end{bmatrix},\qquad [K]=\begin{bmatrix}[K]_{bm} & -[K]_{bm}\\ -[K]_{bm} & [K]_{bm}+[K]_v\end{bmatrix},\qquad \{f(t)\}_a=\begin{Bmatrix}\{f(t)\}_{sa}\\ \{0\}\end{Bmatrix} \quad (3.2)$$

where;

$$[K]_{bm}=\begin{bmatrix} k_{bxx} & k_{bxy} & k_{bxz} & k_{bx\theta x} & k_{bx\theta y} & 0\\ & k_{byy} & k_{byz} & k_{by\theta x} & k_{bx\theta y} & 0\\ & & k_{bzz} & k_{bz\theta x} & k_{bz\theta y} & 0\\ & & & k_{b\theta x\theta x} & k_{b\theta x\theta y} & 0\\ & \text{symmetric} & & & k_{\theta y\theta y} & 0\\ & & & & & 0\end{bmatrix}$$

The stiffness matrices $[K]_{bm}$ and $[K]_V$ pertain to the bearing and mount respectively. The matrices $[M]_S$ and $[M]_C$ are diagonal shaft and casing mass matrices of dimension six respectively.

Lumped parameter technique is used to discretize a simple rotor bearing system to yield Equation (3.1) through the Lagrange's equation of motion

$$\frac{d}{dt}\left(\frac{\partial E_T}{\partial \dot{q}_w}-\frac{\partial E_U}{\partial \dot{q}_w}\right)-\frac{\partial E_T}{\partial q_w}+\frac{\partial E_U}{\partial q_w}+\frac{\partial E_C}{\partial \dot{q}_w}=F_w \qquad w=1,2,3,.... \quad (3.3)$$

where E_T and E_U are the kinetic and potential energies respectively. $E_C = \frac{1}{2}\left\{\dot{q}\right\}^T [C]\left\{\dot{q}\right\}$ is the Rayleigh's dissipation function which is assumed to be ignorable in the following analization. F_W the generalized force. The total system potential energy E_U and kinetic energy E_T are obtained by adding the energies of each of the system components. The partitioned system matrices are:

$$\{q(t)\}_a = \{ \{u(t)\}_{sa}^T \{u(t)\}_{ca}^T \mid \{\theta(t)\}_{Ra}^T \{\theta(t)\}_{ca}^T \mid \{\theta(t)\}_{sa}^T \}^T \quad (3.4\ a)$$

$$[M] = \text{diag} \{ \{m\}_s^T \{m\}_c^T \mid \{I\}_R^T \{I\}_c^T \mid \{I\}_s^T \} \quad (3.4\ b)$$

$$[K] = \begin{bmatrix} [K]_{11} & [K]_{12} & [K]_{13} \\ [K]_{21} & [K]_{22} & [K]_{23} \\ [K]_{31} & [K]_{32} & [K]_{33} \end{bmatrix}, \quad (3.4\ c)$$

where $\{\theta(t)\}_{Ra}$ (subscript R indicates rotor) consists of the alternating angular displacement of all rotors, $\{m\}^T$ and $\{I\}^T$ are the lumped mass and inertia row vectors in a diagonal matrix, with components of the vector corresponding to the diagonal elements. The stiffness submatrices $[K]_{wj}=[K]_{jw}^T$, w,j=1,2,3, consist of the appropriate terms corresponding to the partitioned $\{q(t)\}_a$. For example, $[K]_{11}$ couples $\{\{u(t)\}_{sa}^T \{u(t)\}_{ca}^T\}^T$ degrees of freedom, and $[K]_{12}$ provides a coupling between $\{\{u(t)\}_{sa}^T \{u(t)\}_{ca}^T\}^T$ and $\{\{\theta(t)\}_{Ra}^T \{\theta(t)\}_{ca}^T\}^T$ degrees of freedom.

Assuming the rotary inertia of shaft mass is negligible, reduces the stiffness and mass matrices to;

$$[M] = \text{diag} \{ \{m\}_s^T \{m\}_c^T \mid \{I\}_R^T \{I\}_c^T \} \quad (3.5\ a)$$

$$[K] = \begin{bmatrix} [K]_{11} - [K]_{13}[K]_{33}^{-1}[K]_{31} & [K]_{12} - [K]_{13}[K]_{33}^{-1}[K]_{32} \\ [K]_{21} - [K]_{23}[K]_{33}^{-1}[K]_{31} & [K]_{22} - [K]_{23}[K]_{33}^{-1}[K]_{32} \end{bmatrix}, \quad (3.5\ b)$$

3.1. a *System kinetic energy*

A flexible shaft of length L_S with rigid rotor of mass m_R is subdivided into n_S number of segments of equal length $L_e=L_S/n_S$ with lumped masses at both ends of each segment. Each lumped mass has three translational and three rotational degrees of freedom. The total system kinetic energy E_T is given by $\frac{1}{2}\left\{\dot{q}\right\}^T[M]\left\{\dot{q}\right\}$.

3. 1. b *Shaft stiffness matrix*

Fig.3.1. Lumped parameter model of the flexible shaft. The shaft is divided in to n_s segments. Mass of each segment is equally divided in to each end.

As shown in Fig.3.1 the shaft is divided in to n_s segments. Mass of each segment is assumed to be concentrated on each end of segment equally. Using the direct stiffness approach, the stiffness matrix for one of the shaft segment $[K]_S^e$ of dimension 12 corresponding to the alternating displacement vector $\{q(t)\}_{sa}^e=\{u_{xj+1}(t),\ u_{yj}(t),\ u_{yj+1}(t),\ u_{zj}(t),\ u_{zj+1}(t),\ \theta_{yj}(t),\ \theta_{yj+1}(t),\ \theta_{xj}(t),\ \theta_{xj+1}(t),\ \theta_{zj}(t),\ \theta_{zj+1}(t)\}^T$ of a generic shaft segment is found to be given by

$$[K]_s^e=\begin{bmatrix}[K_{uu}]_s^e & [K_{u\theta}]_s^e\\ [K_{\theta u}]_s^e & [K_{\theta\theta}]_s^e\end{bmatrix}, \qquad (3.6)$$

The non-zero elements of $[K_{uu}]_s^e$, $[K_{u\theta}]_s^e = [K_{\theta u}]_s^e$, $[K_{\theta\theta}]_s^e$ of dimension six are given by the following equations respectively:

$$k_{11}=k_{22}= k_{33}=k_{44}=- k_{12}=- k_{21}=- k_{34}=- k_{43}=12\,EI / L_e^3\,,$$
$$k_{55}=k_{66}=- k_{56}=- k_{65}=AE / L_e\,, \tag{3.7}$$

$$k_{11}=- k_{22}=k_{33}=- k_{44}=k_{12}=- k_{21}=k_{34}=- k_{43}=6EI / L_e^2\,, \tag{3.8}$$

$$k_{11}=k_{22}=k_{33}=k_{44}=4EI / L_e\,, \qquad k_{12}=k_{21}=k_{34}=k_{43}=2EI / L_e\,,$$
$$k_{55}=k_{66}=- k_{56}=- k_{65}=GJ / L_e\ . \tag{3.9}$$

where E is the modulus of elasticity, G is the shear modulus of elasticity, I is the moment of inertia, and J, the polar moment of inertia of the shaft.

The lumped stiffness matrix $[K]_S$ corresponding to $\{q(t)\}_{sa}=\{u_{xj}(t), u_{yj}(t), u_{zj}(t), \theta_{yj}(t), \theta_{xj}(t), \theta_{zj}(t)\}^T$, j=1,2,3,..., for the shaft is constructed by the superposition of all $[K]_s^e$ matrices and merging terms associated with each degree of freedom:

$$[K]_s = \begin{bmatrix} [K_{uu}]_s & [K_{u\theta}]_s \\ [K_{\theta u}]_s & [K_{\theta\theta}]_s \end{bmatrix}, \tag{3.10}$$

The potential energy E_{Us} of the shaft is;

$$E_{U_S} = \frac{1}{2}\{q\}_{sa}^T [K]_s \{q\}_{sa} \tag{3.11}$$

3. 1. c *Flexible Mount Stiffness Matrix*

The flexible mounts are represented by a diagonal stiffness matrix $[K]_V$ corresponding to $\{q(t)\}_{ca}$, which consists of effective stiffness coefficients k_{vw} , $w=x,y,z,\theta_x$,θ_y ,θ_z. Accordingly, the potential energy E_{uv} due to the flexible mounting is

$$E_{U_v} = \frac{1}{2}\{q\}_{ca}^{T}[K]_v\{q\}_{ca} \tag{3.12}$$

3. 1. d *Bearing Stiffness Matrix*

Bearing potential energy is

$$E_{U_b} = \frac{1}{2}\{\delta_{waj},\beta_{waj}\}[K]_{bm}\begin{Bmatrix}\delta_{waj}\\ \beta_{waj}\end{Bmatrix} \tag{3.13}$$

where $\{\delta_{waj},\beta_{waj}\}^T$,w=x,y,z are the bearing displacement vector. These can be expressed in terms of $\{q(t)\}_{saj}$ and $\{q(t)\}_{caj}$ through a coordinate transformation for the jth bearing located at $R_j=\{x_j,y_j,z_j\}$ from the casing center of mass.

3.2. NUMERICAL ESTIMATION OF NATURAL FREQUENCIES

Ignoring damping in the system, simplifies vibration Equation (3.1) in to

$$[K]\, u = \omega^2\, [M]\, u \qquad (3.14)$$

which is an eigenvalue problem where squareroot of the eigen values are natural frequencies. Introducing the transformation

$$u = [M]^{-1/2}\, x \qquad (3.15)$$

in to Equation (3.14) and premultiplying the result by $[M]^{-1/2}$ will give

$$[M]^{-1/2}\, [K]\, [M]^{-1/2}\, x = \omega^2\, x \qquad (3.16)$$

Hence the eigenvalue problem reduces to the form $[A]\, x = \lambda\, x$ where,

$$[A] = [M]^{-1/2}\, [K]\, [M]^{-1/2} \qquad (3.17)$$

One of the numerical methods to estimate eigen values is Jacobi method. This is an iterative method which produces all of the eigenvalues and eigenvectors of [A] where [A] is a real symmetric matrix. However, all of the eigen values can not be precisely computed. Computational error increases for higher eigen values. The method uses similarity transformations to diagonalize matrix [A] where the diagonal elements are simply the eigenvalues. The transformation is made by the rotation matrix [R] which has the form:

$$[R] = \begin{bmatrix} \mathrm{Cos}\theta & -\mathrm{Sin}\theta \\ \mathrm{Sin}\theta & \mathrm{Cos}\theta \end{bmatrix} \qquad (3.18)$$

This is an orthonormal matrix as it satisfies $[R]^T\, [R]=[R][R]^T = [\, I\,]$. The diagonal matrix [A] has the form

$$[\Lambda] = [R]^T [A][R] \qquad (3.19)$$

The iteration sequence is given by

$$[A]_k = [R]_k{}^T [A]_{k-1} [R]_k \qquad k=1,2,3,..... \qquad (3.20)$$

where $[A]_0 = [A]$. Assuming the off diagonal element of $[A]_{k-1}$ is in the (p,q) position, the rotation matrix $[R]_k$ can be exhibited in the form

$$R_k = \begin{array}{c} \\ \\ \\ \\ \\ \\ \\ \end{array} \begin{array}{c} \begin{array}{ccccccccc} & & & & p & & q & & \end{array} \\ \begin{bmatrix} 1 & 0 & . & 0 & . & 0 & . & 0 \\ 0 & 1 & . & 0 & . & 0 & . & 0 \\ . & & & & & & & \\ 0 & 0 & . & \cos\theta_k & . & -\sin\theta_k & . & 0 \\ . & . & . & . & . & . & . & . \\ 0 & 0 & . & \sin\theta_k & . & \cos\theta_k & . & 0 \\ . & . & . & . & . & . & . & . \\ 0 & 0 & . & 0 & . & 0 & . & 1 \end{bmatrix} \end{array} \begin{array}{c} \\ \\ \\ p \\ \\ q \\ \\ \end{array}$$

where,

$$\tan 2\theta_k = \frac{2a_{pq}^{(k-1)}}{a_{pp}^{(k-1)} - a_{qq}^{(k-1)}} \qquad (3.21)$$

Numerical application of Jacobi method for one of the example cases is given in App. 1.

4. EXPERIMENTAL RESULTS

4. 1. EXPERIMENTAL PROCEDURE

The theory described will be now applied to the system shown in Fig.4.1. Physical model is shown in Fig.4.2. Angular contact type ball bearings are used in pedestals 1 and 2, deepgroove type of ball bearing is used in pedestal 3. Related parameters of these bearings are given in Table 4.1. X type of adjustment is made which means that angular contact type of bearings are face to face, so there is no need to give high preloads to the bearings.

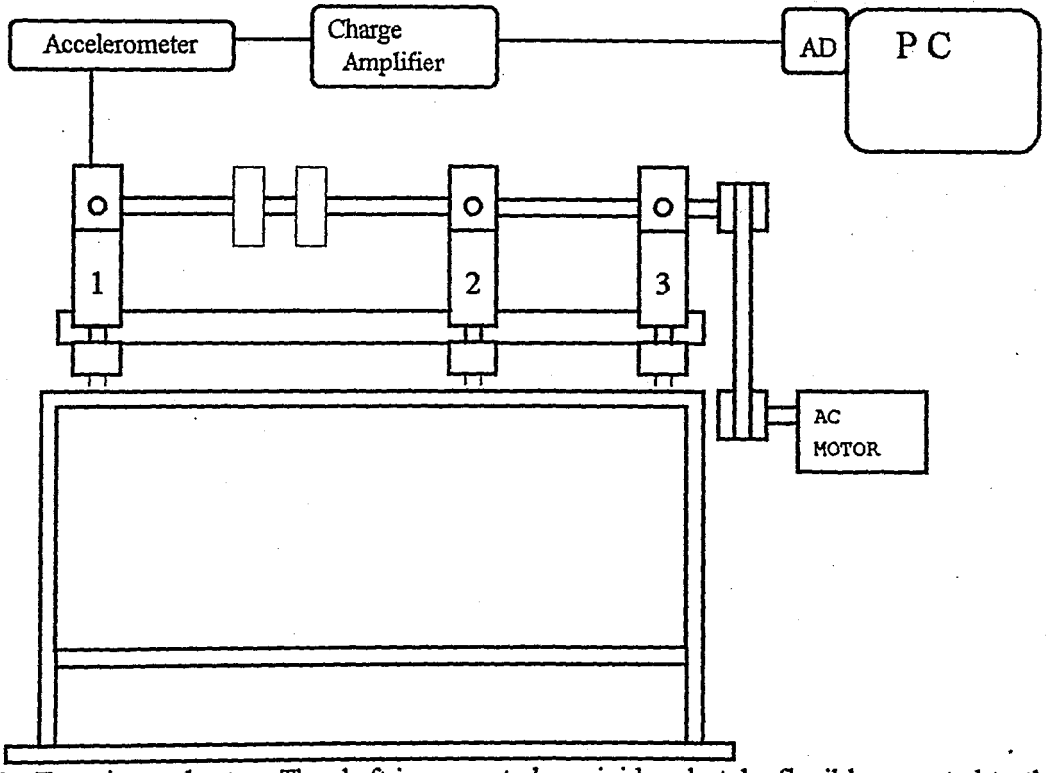

Fig. 4.1 Experimental setup. The shaft is supported on rigid pedestals, flexibly mounted to the rigid table, which is on a flexible foundation.

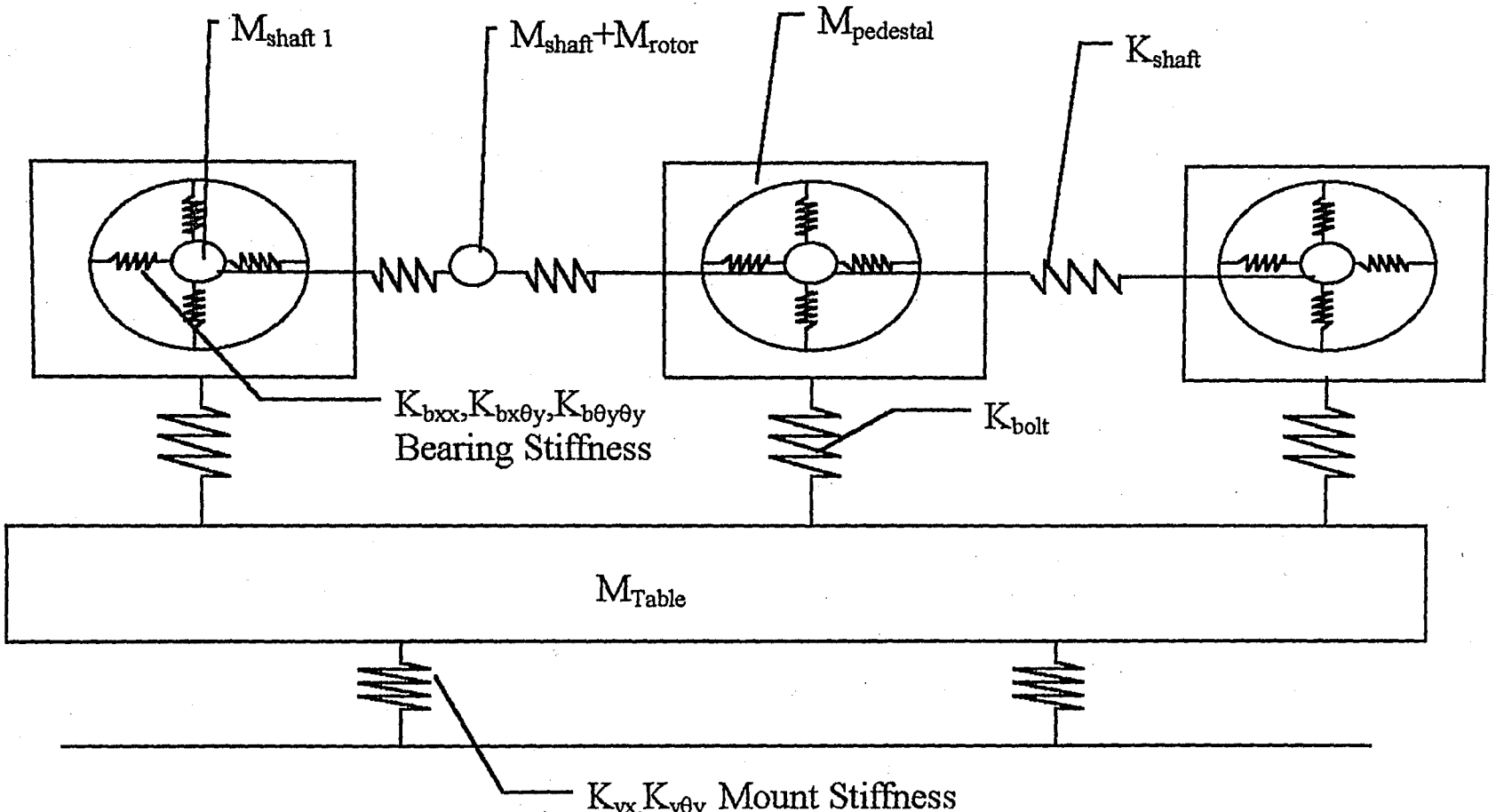

Figure. 4.2 Physical model of the experimental system.

Table 4.1
Design parameters for ball bearing types used in experimental setup are requested from FAG, Germany.

Parameters	
Type	FAG 7204 B Angular contact ball bearing
Load-deflection constant K_n (N/m^n)	5.38 E+10
Number of rolling elements, Z	11
Radial clearance, r_Γ, (mm)	.00002-.0005
Pitch radius, r_i (mm)	25.5
A_0 (mm)	0.4366
Type	FAG 6204 Deep groove ball bearing
Load-deflection constant K_n (N/m^n)	5.16 E+10
Number of rolling elements, Z	11
Radial clearance, r_Γ, (mm)	.00002-.0005
Pitch radius, r_i (mm)	25.5
A_0 (mm)	0.334

Actually it is not very easy to determine the exact value of the preload on the bearings acting in such a system. To compute $[K]_{bm}$ we either need mean displacement of the bearings or the preload on the bearings. Due to this reason, an axial preload range for the bearings will be assumed.

4. 1. a Single rotor case :

As a first example we will study the case of a system with single rotor. This is achieved by placing the rotors next to each other at the middle of the shaft, (Fig 4.3). The shaft is divided into three segments.

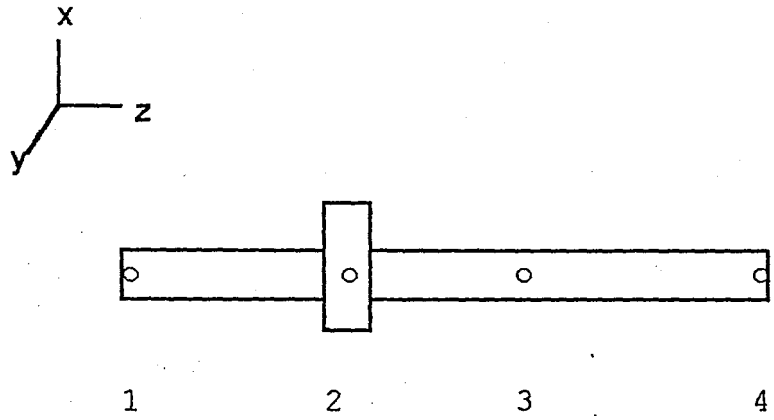

Fig. 4.3 Lumped parameter model of the flexible shaft with single rigid rotor. The shaft is supported by bearings at node 1, 3 and 4.

Lumped masses are assumed to be divided at each end of the segment. Bearings are located at 1^{st} ,3^{rd} and 4^{th} nodes. The system parameters are as given in Table 4.2.

The effective bearing stiffness constants corresponding to an axial mean load are k_{bxx}, k_{byy}, k_{bzz}, $k_{b\theta x\theta x}$, $k_{b\theta y\theta y}$, $k_{bx\theta y}$, $k_{by\theta x}$. The vibration equation may be simplified to a two dimensional vibrating system in the x-y plane; due to the absence of coupling between the torsional and transverse motions of the shaft and due to the absence of external force $F_{zba}(t)$. The dynamics associated with $\{u_{zsaj}, u_{zca}, \theta_{zRa}(t)\}^T$, (j is a dummy index to identify the shaft lumped masses) are decoupled from others and have trivial, steady-state particular solution. Now there is two sets of uncoupled differential equations, one set is $\{u_{xsaj}, u_{xca}, \theta_{yRa}(t), \theta_{ypai}(t)\}^T$ which is forced by $F_{xsa}(t)$; and the other is

$\{u_{xsaj}\ ,\ u_{xca}\ ,\ \theta_{yRa}(t),\ \theta_{ypai}(t)\}^T$ forced by $F_{ysa}(t)$. These two sets of equations are similar and independent and result in the synchronus whirling motion of the rotating shaft. Analization of the vibration induced by $F_{xsa}(t)$ will be given in detail here and due to the similarity only the results of the other one, will be stated. System matrices for the vibration in x-direction in partitioned form will be as:

$$\{q(t)\}_a = \{u_{xsaj}(t),\ u_{xpia}(t),\ u_{xTa}(t),\ \big|\ \theta_{yRa}(t),\ \theta_{ypia}(t),\ \theta_{yTa}(t)\ ,\ \big|\ \theta_{ysa}(t)\}^T$$

$$[M] = \text{diag}\{\{m\}^T_{sj},\ \{m\}^T_{pi},\ m_T,\ \big|\ I_{yR},\ \{I\}^T_{ypi},\ I_{yT},\ \big|\ \{I\}^T_{ysj}\}\ ,\ i=1,2,3;\ j=1,2,\ldots 4$$

$$[K] = \begin{bmatrix} [K]_{11} & [K]_{12} & [K]_{13} \\ [K]_{21} & [K]_{22} & [K]_{23} \\ [K]_{31} & [K]_{32} & [K]_{33} \end{bmatrix}$$

Degrees of freedom is 16 now, neglecting the shaft inertia will result in 13 DOF and

$$\{q(t)\}_a = \{u_{xsaj}(t),\ u_{xpia}(t),\ u_{xTa}(t),\ \theta_{yRa}(t),\ \theta_{ypia}(t),\ \theta_{yTa}(t)\}^T .$$

Resulting partitioned mass, and stiffness matrices will be as

$$[M] = \text{diag}\{\{m\}^T_{sj},\ \{m\}^T_{pi},\ m_T\ \big|\ I_{yR},\ \{I\}^T_{ypi},\ I_{yT}\}\ ,\ \ I=1,2,3;\ \ j=1,2,\ldots 4$$

$$[K] = \begin{bmatrix} [K]_{11} - [K]_{13}[K]_{33}^{-1}[K]_{31} & [K]_{12} - [K]_{13}[K]_{33}^{-1}[K]_{32} \\ [K]_{21} - [K]_{23}[K]_{33}^{-1}[K]_{31} & [K]_{32} - [K]_{23}[K]_{33}^{-1}[K]_{32} \end{bmatrix}$$

Detailed [K] and [M] matrices are given in App.2.

The theoretical undamped natural frequencies calculated by Jacobi method of the single rotor-bearing system for the vibration in x-direction are given in Table 4.3. Results of the analysis in y-direction are given in App.3.

Table 4.2
System parameters of the experiment.

Rotor mass, m_R (kg) and mass moment of inertias, I_{yR} (kg m^2), I_{xR} (kg m^2)	1.3, .89E-3, .89E-3
Shaft mass, m_s (kg) and length, L_s (m)	1.435, .51
Pedestal mass, m_p (kg) and mass moment of inertias, I_{yp} (kg m^2), I_{xp} (kg m^2)	8.5, 8.52E-3 ,1.96E-2
Table mass, m_T (kg) and mass moment of inertia, I_{yT} (kg m^2), I_{xT} (kg m^2)	25, 2.54, 2.54
Shaft flexural rigidity, EI (N m^2)	1.492E+3
Bearing axial preload range, F_{zbm} (N)	5 - 15
kbxx,kbxθ_y, kb$\theta_y\theta_y$ (for the bearings in pedestals 1 and 2)	4.5E+7, -9.68E+5,2.07E+4
kbxx,kbxθ_y, kb$\theta_y\theta_y$ (for the bearing in pedestal 3)	2.07E+8, -1.74E+5, 1.923E+3
kvx, kvθy	9E+4, 7.78E+4
kbx,kbθ_y	7.46E+8, 4.663E+3

Table 4.3
Natural frequencies (Hz) of the single rotor system
for the vibration in the x-direction.

1	6.5
2	20
3	75
4	78
5	79
6	160
7	860
8	1396
9	1480
10	1654
11	1761
12	2129
13	4925

Corresponding modal matrix where columns are the modal vectors is :

$$\begin{bmatrix}
0.14 & -0.15 & 0.08 & -0.01 & -0.13 & 0.17 & -0.16 & -0.99 & 1.70 & 0.03 & -0.65 & 0.17 & 0.00 \\
0.14 & -0.08 & 0.14 & -0.01 & 0.07 & -0.53 & 0.02 & -0.03 & 0.01 & -0.02 & -0.02 & 0.00 & 0.00 \\
0.14 & 0.01 & 0.09 & 0.00 & 0.12 & -0.03 & -0.39 & 0.73 & 0.45 & 1.10 & 0.25 & 0.14 & 0.00 \\
0.14 & 0.11 & 0.00 & -0.01 & 0.00 & 0.02 & 0.02 & -0.11 & -0.12 & 0.17 & -0.16 & -0.15 & 2.08 \\
0.14 & -0.13 & -0.03 & 0.01 & -0.01 & 0.04 & 0.01 & -0.09 & 0.02 & 0.01 & 0.22 & -0.15 & 0.00 \\
0.14 & 0.03 & -0.01 & 0.00 & 0.00 & 0.03 & -0.01 & 0.20 & 0.08 & -0.15 & -0.09 & -0.15 & 0.00 \\
0.14 & 0.11 & 0.00 & -0.01 & 0.00 & 0.02 & 0.01 & -0.11 & -0.11 & 0.15 & -0.14 & -0.12 & -0.06 \\
0.14 & 0.01 & -0.01 & 0.00 & 0.00 & 0.03 & 0.00 & 0.00 & -0.02 & -0.02 & 0.01 & 0.14 & 0.00 \\
0.00 & -0.44 & -0.05 & -0.02 & -0.84 & 0.29 & 22.73 & 3.33 & 3.83 & 4.26 & 0.12 & 0.64 & -0.07 \\
0.00 & 0.54 & -5.49 & 0.96 & 4.30 & -0.91 & 0.12 & -0.28 & 0.51 & 0.02 & -0.19 & 0.05 & 0.00 \\
0.00 & 0.46 & -3.97 & 0.13 & -5.56 & -1.94 & -0.34 & 0.29 & 0.17 & 0.46 & 0.11 & 0.06 & 0.01 \\
0.00 & 0.48 & 0.91 & 7.06 & -0.46 & 0.04 & 0.00 & 0.00 & 0.00 & 0.00 & 0.00 & 0.00 & 0.02 \\
0.00 & 0.46 & 0.06 & -0.04 & 0.01 & -0.05 & 0.01 & -0.05 & 0.11 & -0.07 & 0.24 & -0.01 & 0.00
\end{bmatrix}$$

Modal shapes for the first three modes are given in Fig. 4.4, where first mode represents a rigid body motion with 6.5 Hz.

Accelerations of pedestals are measured by Brüel & Kjaer 4283 type of accelerometer which converts acceleration in to charge. By Kistler 5037A2221 type of charge amplifier, the charge coming from the accelerometer is converted in to Volt for the AD card.

Comparison of experimental and theoretical results are shown in Fig. 4.5 and Fig. 4.6 Critical frequencies are at 6.5 Hz, 18 Hz., 65 Hz. Discrepancies between Jacobi method is due to decreased precision of numeric methods for higher eigen values as stated above. Experimental results seem to be in agreement with the theoretical ones. It should be noted that the analizations are made by assuming the system to be undamped, but actually there is some damping in the system. This is an important reason for the discrepancies between the theoretical and experimental results. Actually the excitation coming from the motoring unit is not easy to predict precisely. Assumption of this effect brings an other error for the calculations.

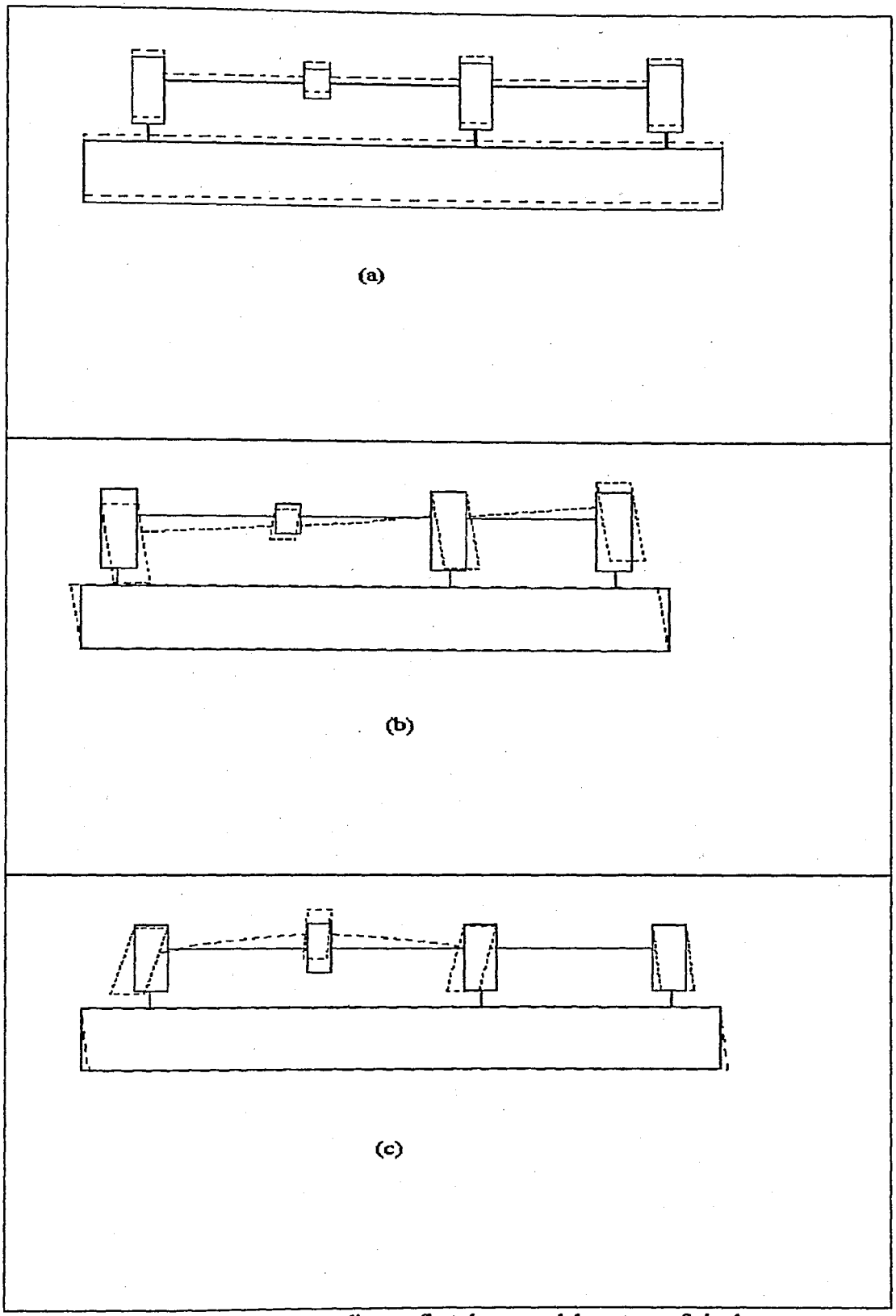

Fig. 4.4. Modal shapes corresponding to first three modal vectors of single-rotor system. (a) First modal shape vibrating with 6.5 Hz. (b) Second modal shape vibrating with 20 Hz. (c) Third modal shape vibrating with 75 Hz.

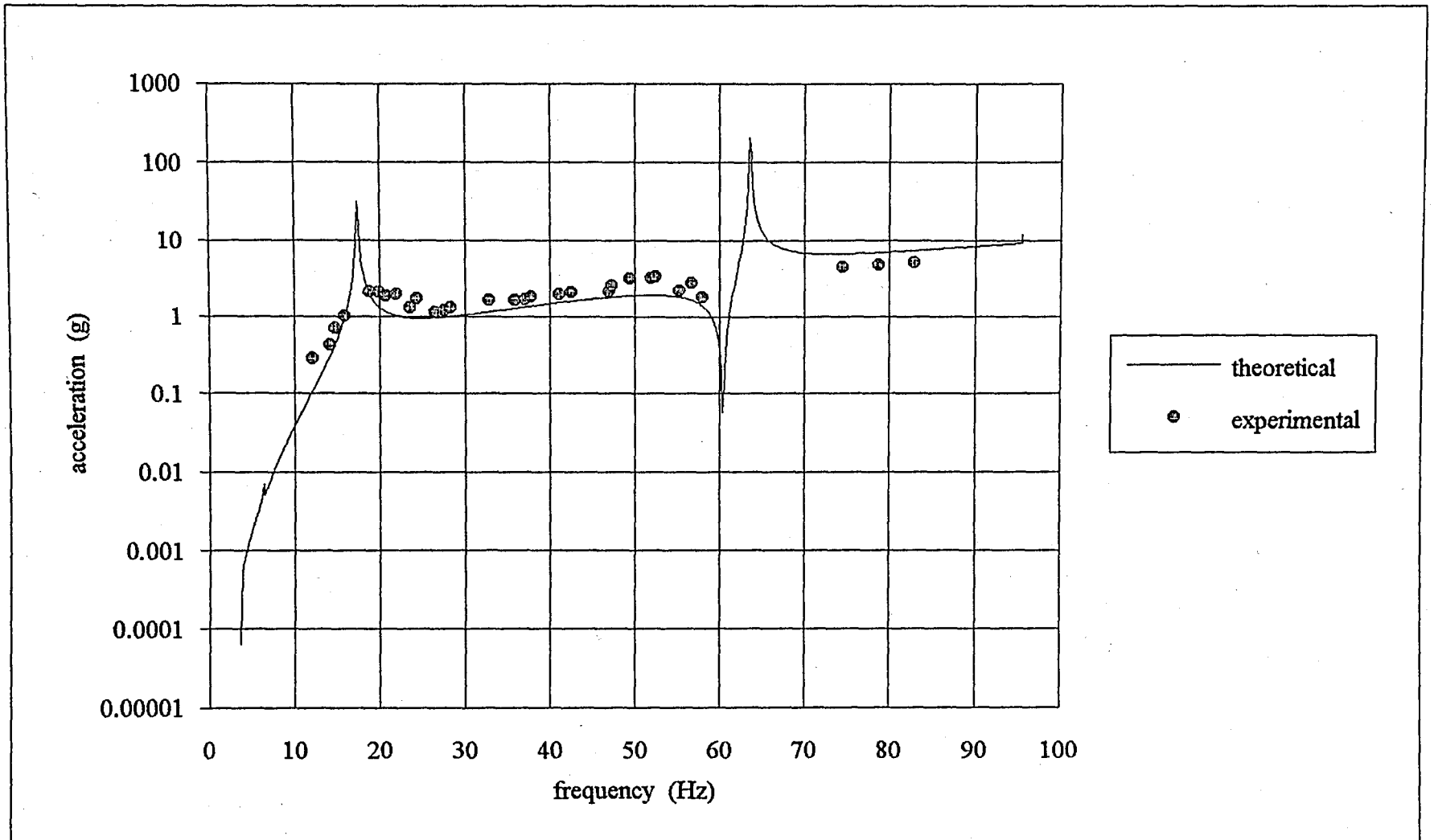

Figure 4.5. Comparison of theoretical and experimental results in the x-direction of pedestal 1 in single rotor system . Accelerations are normalized with respect to g.

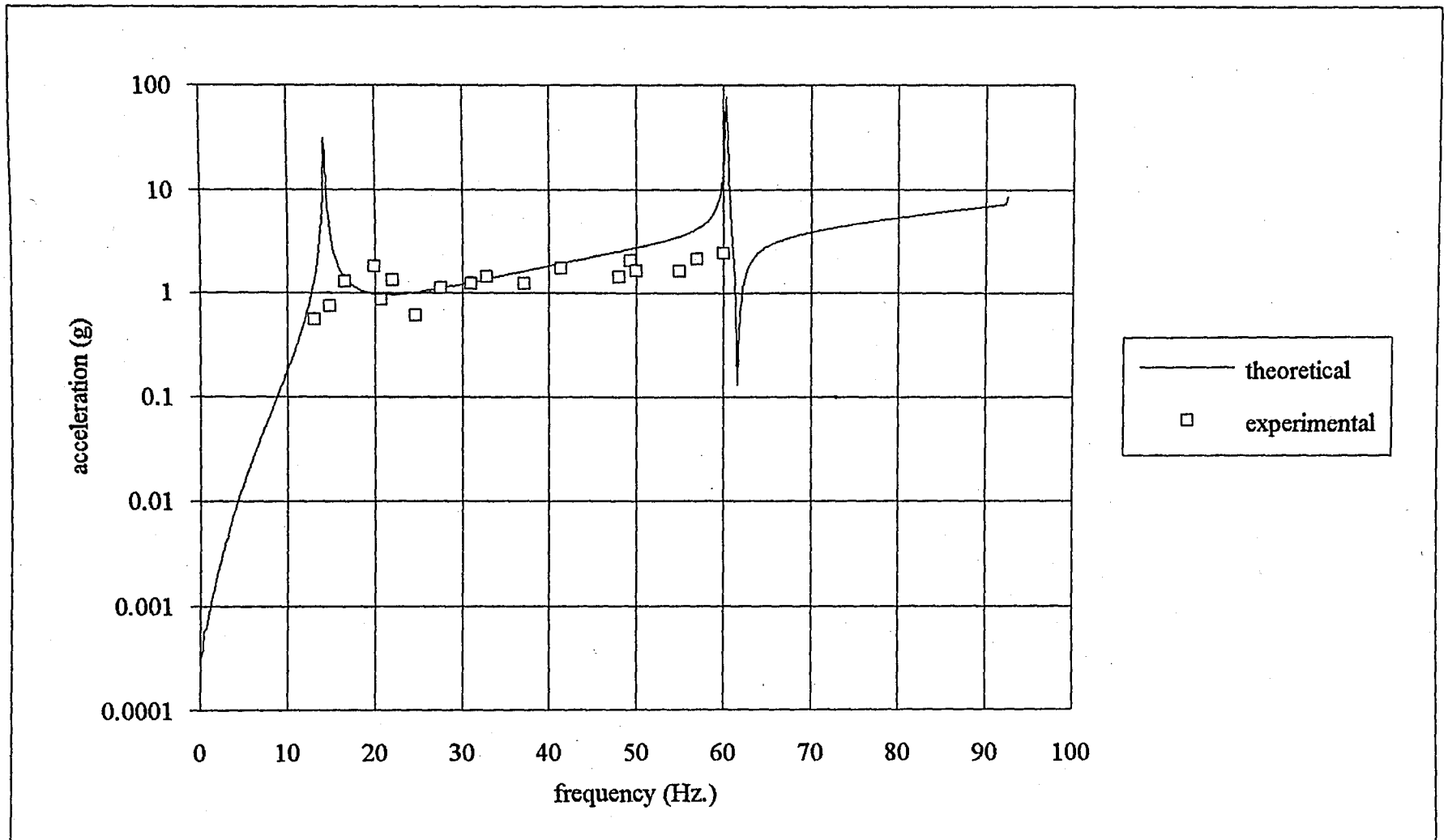

Figure 4.6. Comparison of theoretical and experimental results in the x-direction of pedestal 2 in single rotor system. Accelerations are normalized with respect to g.

4.1. b Double rotor case :

As a secondl example the rotors were placed 0.125m apart from each other. In this case the number of increased to four parts, Fig. 4.7.

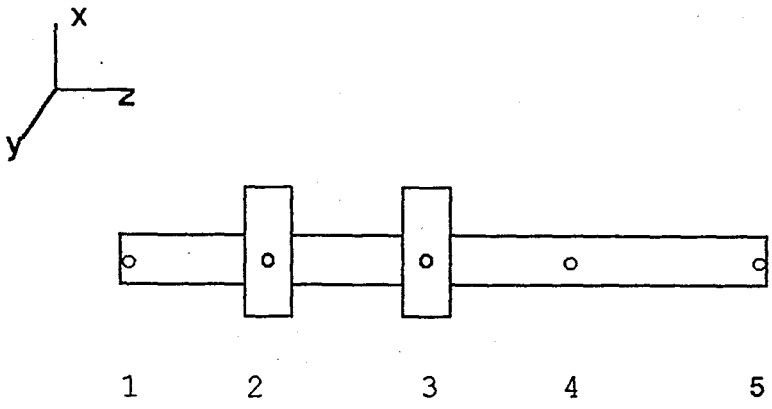

Fig 4.7 The system is reanalyzed by placing rotors apart from each other.

Masses were again assumed to be equally divided and located at each end of the segment.

Degrees of freedom of the system is 15 now due to the increased number of segments and the undamped natural frequencies of corresponding system calculated by Jacobi method for the vibrattion in the x-direction, are given in Table 4.4.

Table 4.4
Natural frequencies (Hz) of the double rotor system for the vibration in x-direction

1	6.5
2	22
3	76
4	143
5	366
6	375
7	559
8	1302
9	1476
10	1647
11	1790
12	1835
13	2112
14	2288
15	5698

Corresponding Modal matrix is:

$$\begin{bmatrix}
0.14 & -0.15 & -0.14 & -0.18 & -0.01 & -0.11 & 0.08 & -0.04 & 0.53 & -1.76 & -0.46 & -1.44 & 0.37 & 0.03 & 0.00 \\
0.14 & -0.11 & -0.10 & 0.43 & 0.03 & 0.42 & -0.42 & -0.11 & 0.01 & -0.01 & -0.09 & -0.03 & 0.02 & -0.03 & 0.00 \\
0.14 & -0.06 & -0.05 & 0.57 & -0.01 & -0.17 & 0.46 & 0.00 & 0.06 & -0.03 & 0.14 & 0.00 & 0.01 & -0.05 & 0.00 \\
0.14 & 0.01 & -0.01 & 0.21 & -0.05 & -0.53 & -0.15 & -0.47 & -0.25 & 0.09 & -0.48 & -0.10 & -0.44 & 1.37 & -0.02 \\
0.14 & 0.11 & -0.01 & -0.02 & -0.03 & -0.01 & -0.02 & 0.05 & 0.16 & 0.15 & -0.01 & -0.16 & -0.15 & -0.02 & 2.41 \\
0.14 & -0.13 & 0.02 & -0.05 & 0.00 & -0.01 & 0.00 & 0.02 & 0.10 & -0.11 & -0.04 & 0.17 & -0.15 & -0.03 & 0.00 \\
0.14 & 0.03 & 0.00 & -0.03 & 0.00 & 0.00 & 0.01 & -0.05 & -0.26 & -0.04 & 0.04 & -0.07 & -0.11 & -0.10 & 0.00 \\
0.14 & 0.12 & -0.01 & -0.02 & 0.00 & 0.00 & -0.01 & 0.04 & 0.16 & 0.14 & -0.01 & -0.14 & -0.12 & -0.03 & -0.05 \\
0.14 & 0.01 & 0.01 & -0.03 & 0.00 & 0.00 & 0.00 & 0.01 & -0.01 & 0.01 & 0.01 & 0.03 & 0.13 & 0.04 & 0.00 \\
0.00 & -0.36 & -0.35 & -3.67 & 0.03 & 0.25 & -3.88 & 19.41 & 8.11 & -3.21 & 25.04 & -0.66 & -1.72 & 3.40 & 0.00 \\
0.00 & -0.51 & -0.40 & 1.52 & 0.54 & 6.48 & -2.52 & 23.49 & -3.37 & -5.69 & 16.04 & -2.06 & -5.91 & 13.43 & -0.22 \\
0.00 & 0.61 & 7.01 & 1.02 & 0.03 & 0.37 & -0.29 & -0.15 & 0.16 & -0.40 & -0.01 & -0.33 & 0.08 & 0.01 & 0.00 \\
0.00 & 0.30 & 0.37 & -6.63 & 2.36 & 24.01 & 19.21 & -6.33 & -0.39 & 1.22 & -4.11 & -0.50 & -2.39 & 7.97 & 0.15 \\
0.00 & 0.48 & -0.07 & 0.18 & 33.38 & -3.03 & -0.25 & 0.03 & 0.01 & 0.03 & 0.01 & -0.04 & -0.03 & 0.00 & 0.38 \\
0.00 & 0.46 & -0.05 & 0.06 & 0.00 & 0.03 & -0.02 & -0.02 & 0.03 & -0.20 & -0.04 & -0.17 & -0.02 & 0.00 & 0.00
\end{bmatrix}$$

where each column represents a modal vector. Modal shapes are given in Fig. 4.8. As in the single rotor case first modal vector represents a rigid body motion of the whole system, with 6.5 Hz.

Comparison of theoretical and experimental results are shown in Fig. 4.9and Fig. 4.10. Critical values occur at 16 Hz and 62 Hz, which correspond to 22 Hz and 76 Hz. found in Jacobi method. 62 Hz. can not be seen as critical frequency for the first pedestal. First pedestal is a nodal point for the mode corresponding to this frequency, as can be seen from the corresponding modal shape. The decreased precision of the numeric methods for eigen value problems as eigen value increases may be a reason for the difference of the natural frequencies as stated above. The discrepancies between the results may be due to theoretical and experimental errors. The theoretical errors are mostly due to damping effect in the system which is ignored in our analysis, and due to the motoring effect which is not easy to predict precisely as in the case of single rotor system. The measurement system is not quite sensitive actually, this may be the reason for the experimental errors.

Bearing force and moment transmissibilities are calculated by normalizing transmitted force by shaft unbalance force and shown in Figures 4.11-4.16. The results presented are only for the angular contact type of ball bearing used in pedestal 1. As bearing force transmissibility, for the single rotor system simple model predicts lower transmissibility with respect to this model; and for the double rotor system, predicts a lower critical frequency for the one around 76 Hz. Same effect can be seen in the mount force transmissibility curve for the double rotor system. For the single rotor system, simple model predicts same mount force transmissibility as this model. Bearing moment transmissibility is not predicted by simple models. This component of the bearing transmissibility spectra is primarily due to coefficients $k_{bx\theta y}$, $k_{b\theta y\theta y}$ which are obviously not included in simple models.

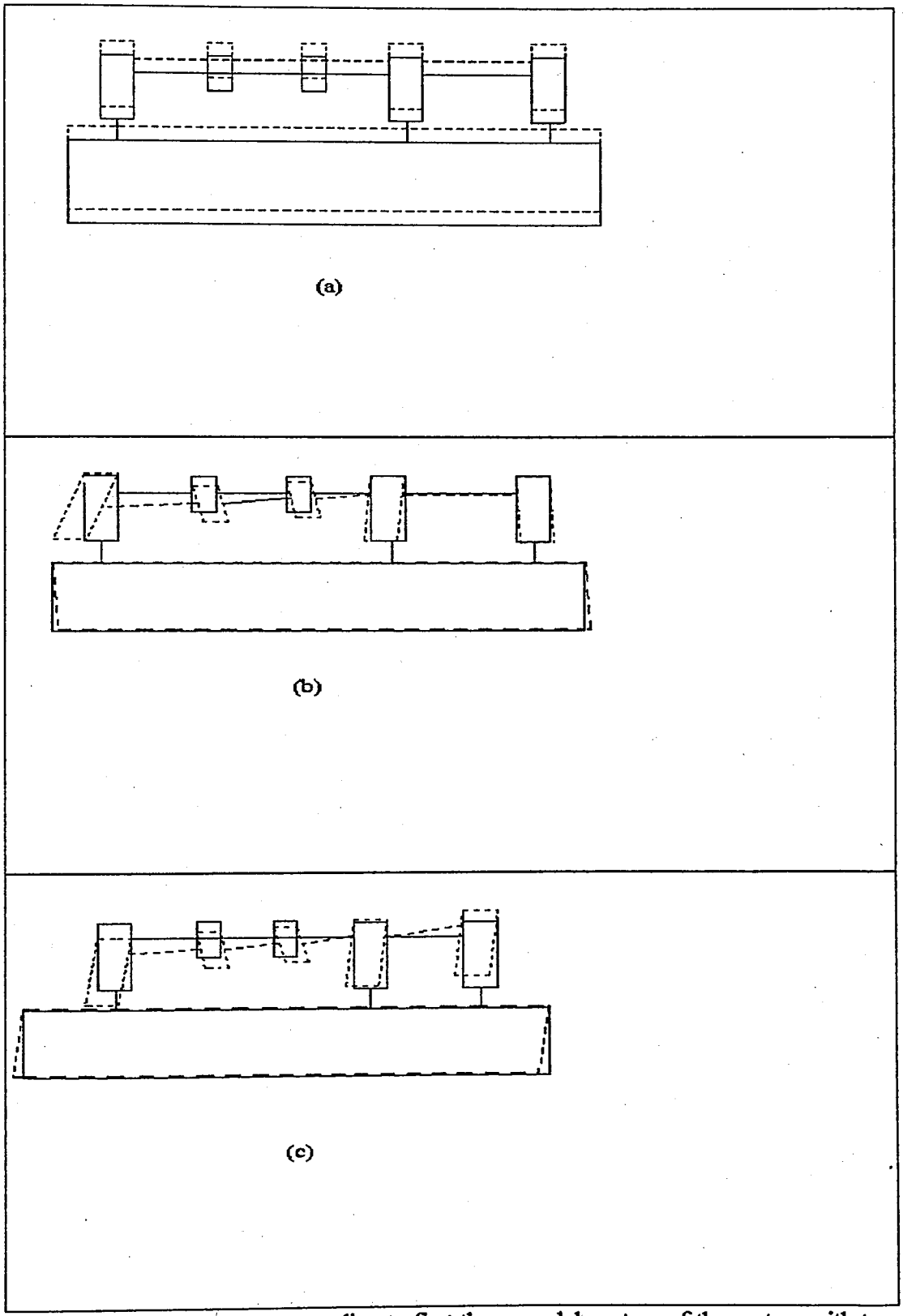

Fig.4.8. Modal shapes corresponding to first three modal vectors of the system with two rotors. (a) First modal shape vibrating with 6.5 Hz. (b) Second modal shape vibrating with 22 Hz. (c) Third modal shape vibrating with 76 Hz.

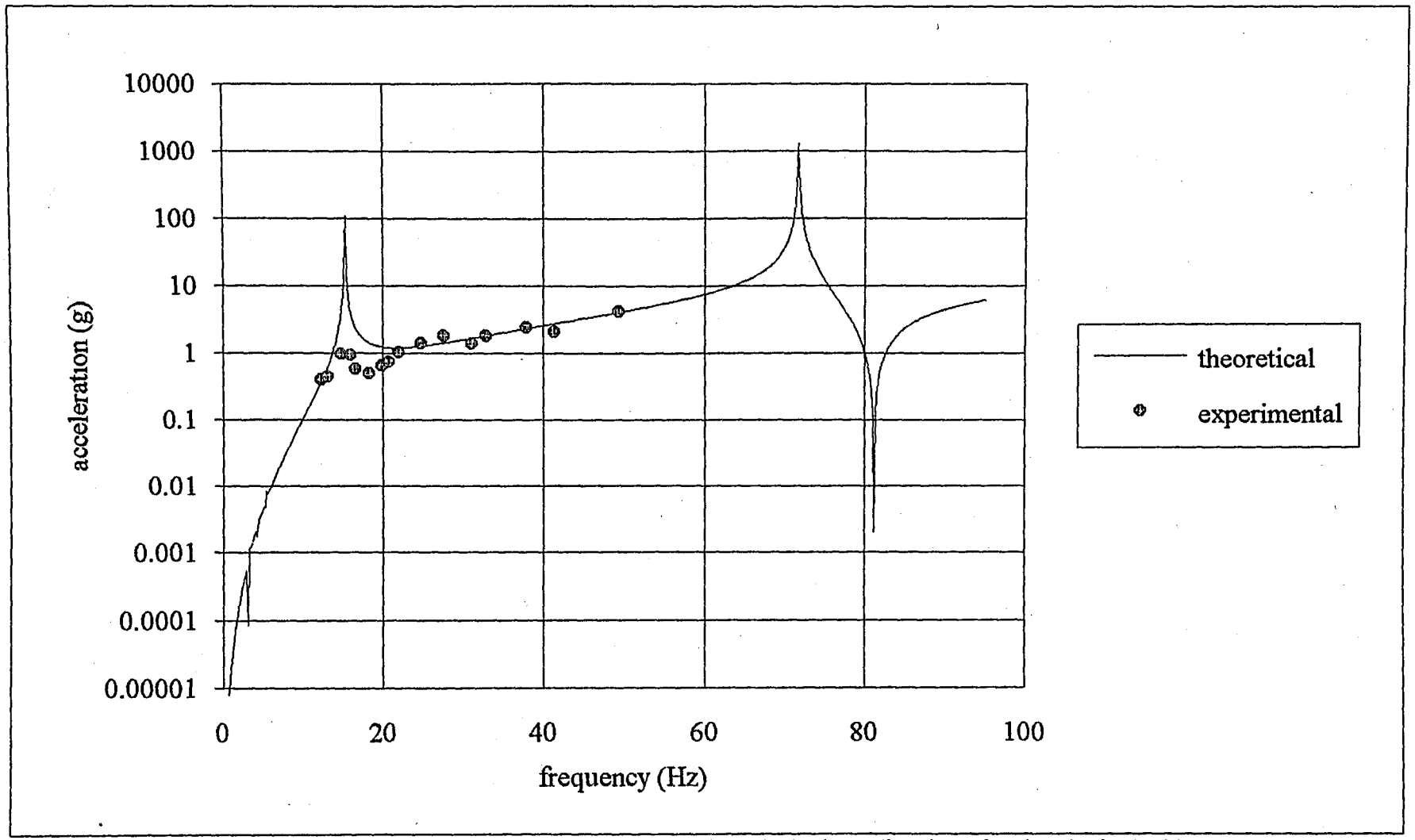

Fig. 4.9. Comparison of theoretical and experimental results in the x-direction of pedestal 1 in double-rotor system. Accelerations are normalized with respect to g.

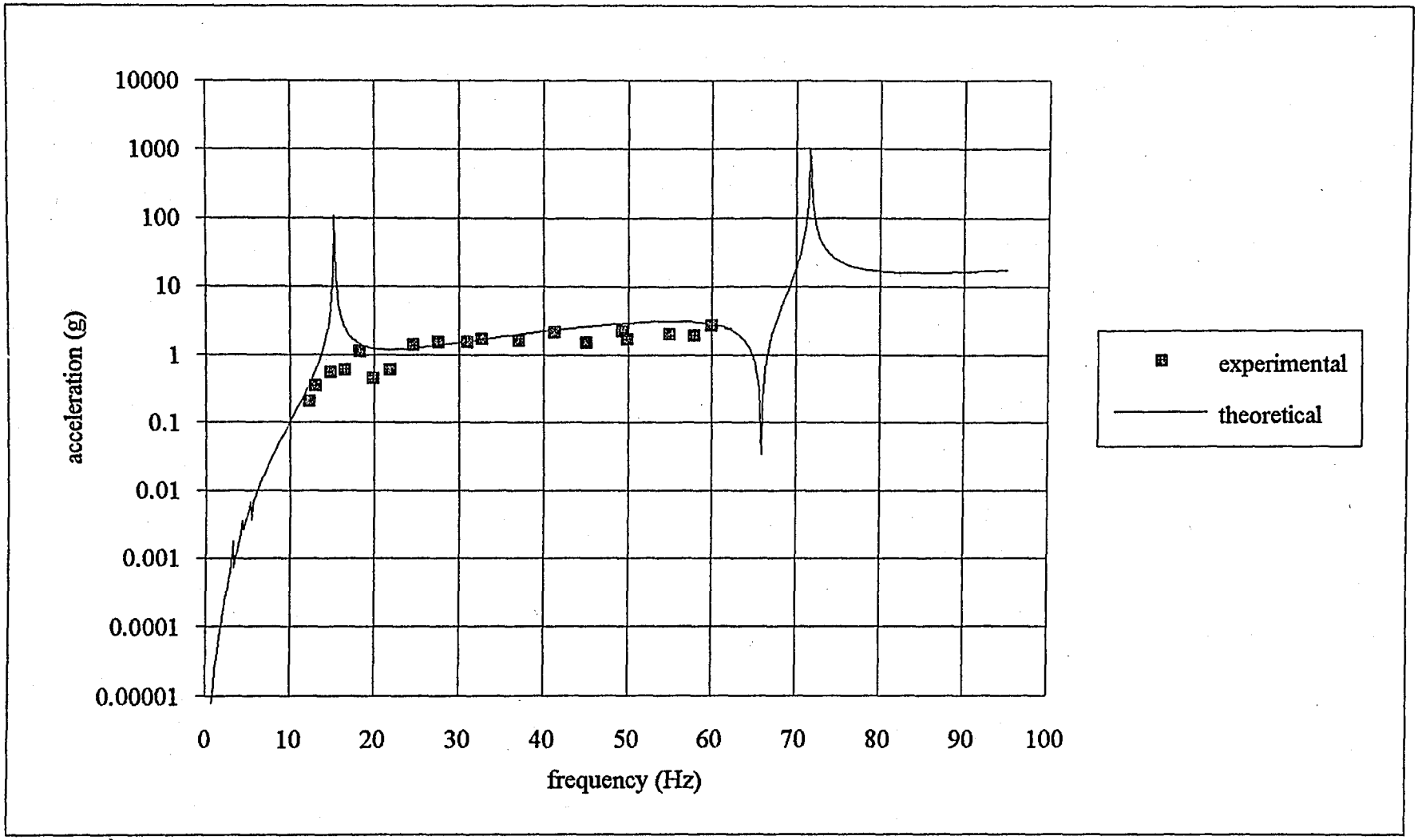

Fig. 4.10. Comparison of theoretical and experimental results in the x-direction of pedestal 2 in double-rotor system. Accelerations are normalized with respect to g.

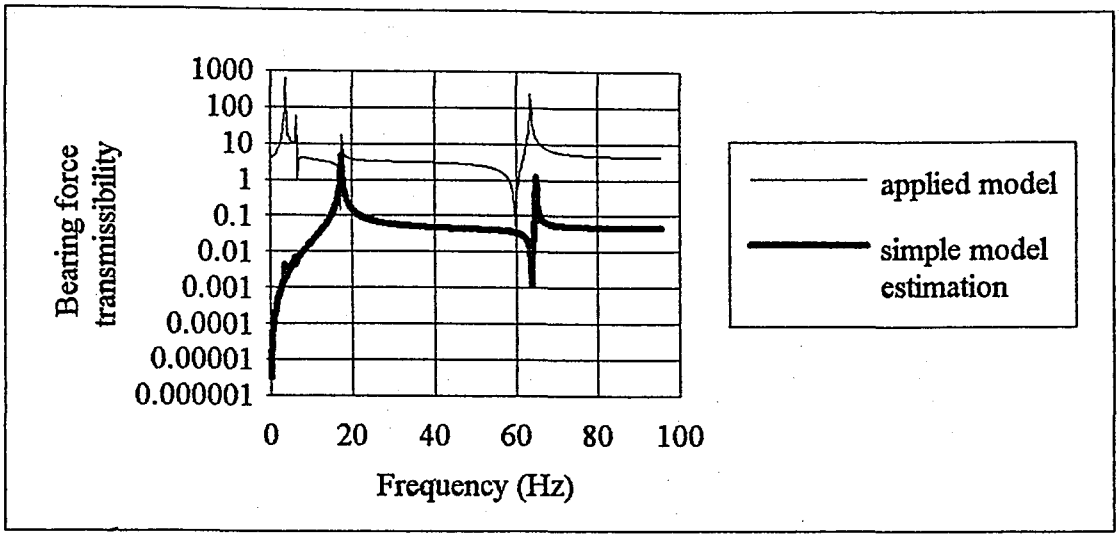

Fig. 4.11. Bearing force transmissibility, for the single rotor case normalized with respect to the unbalance force on the shaft.

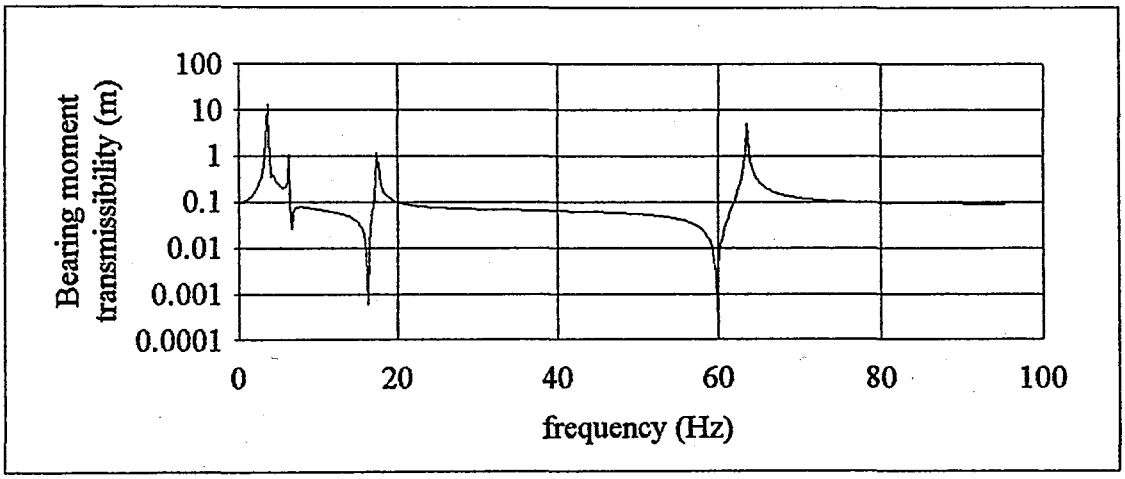

Fig. 4.12. Bearing moment transmissibility, for the single-rotor system normalized with respect to the unbalance force on the shaft.

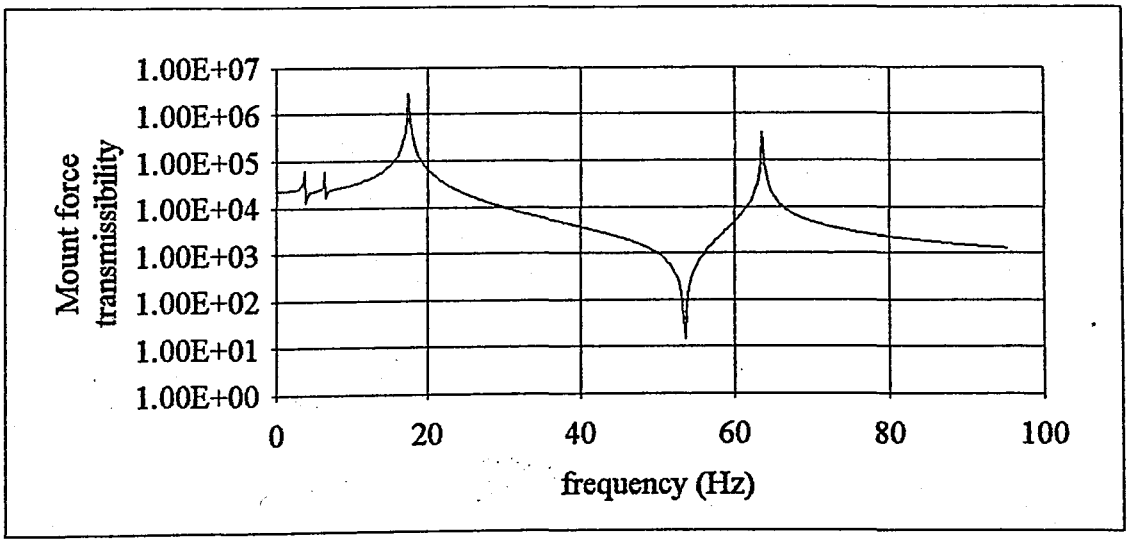

Fig. 4.13. Mount force transmissibility, for single rotor case normalized with respect to the unbalance force on the shaft.

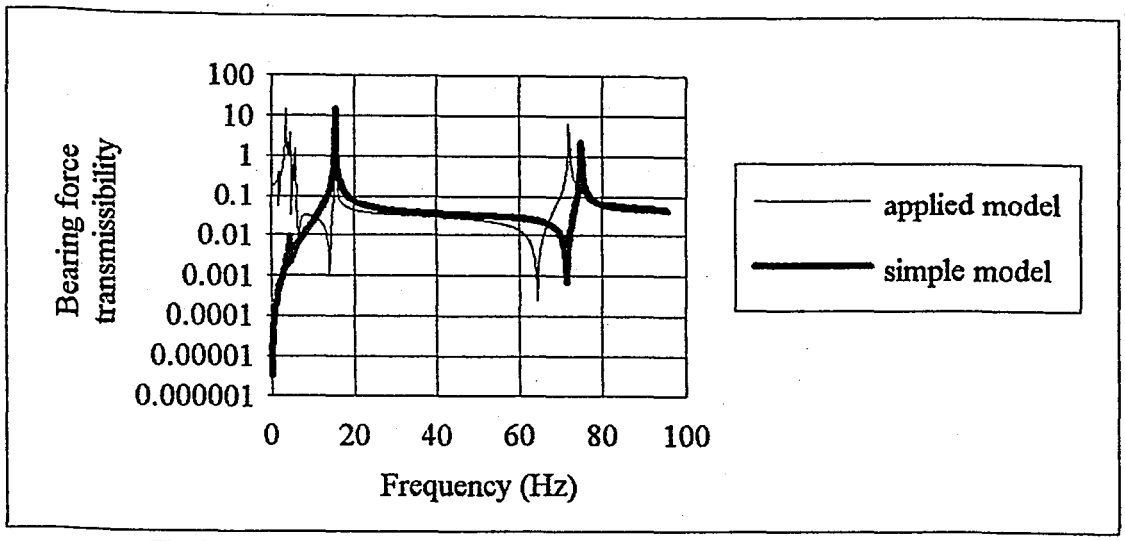

Fig.4.14. Bearing force transmissibility for double-rotor system normalized with respect to the unbalance force on the shaft.

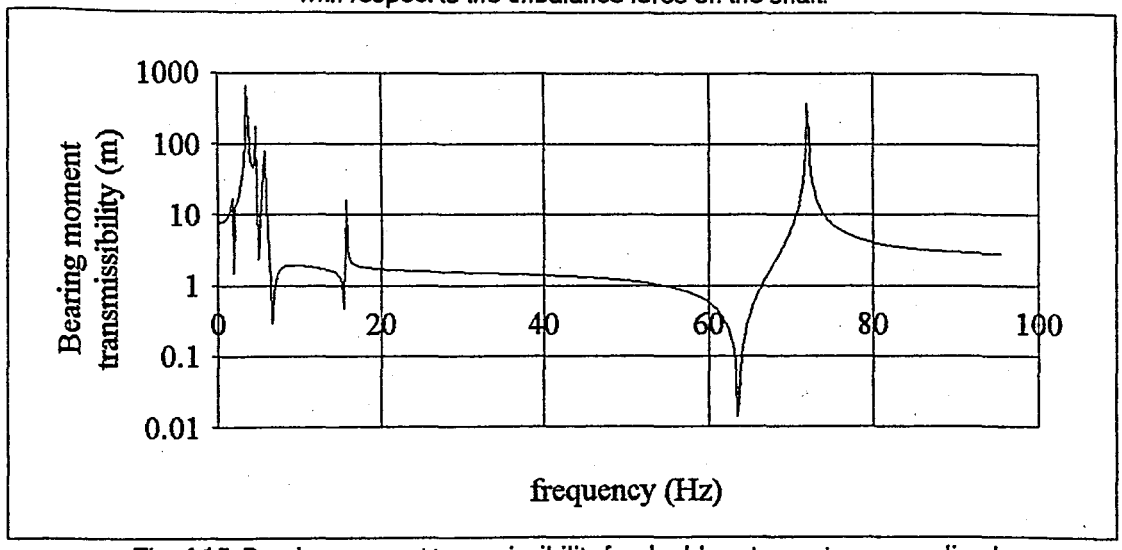

Fig. 4.15. Bearing moment transmissibility for double-rotor system normalized with respect to the unbalance force on the shaft.

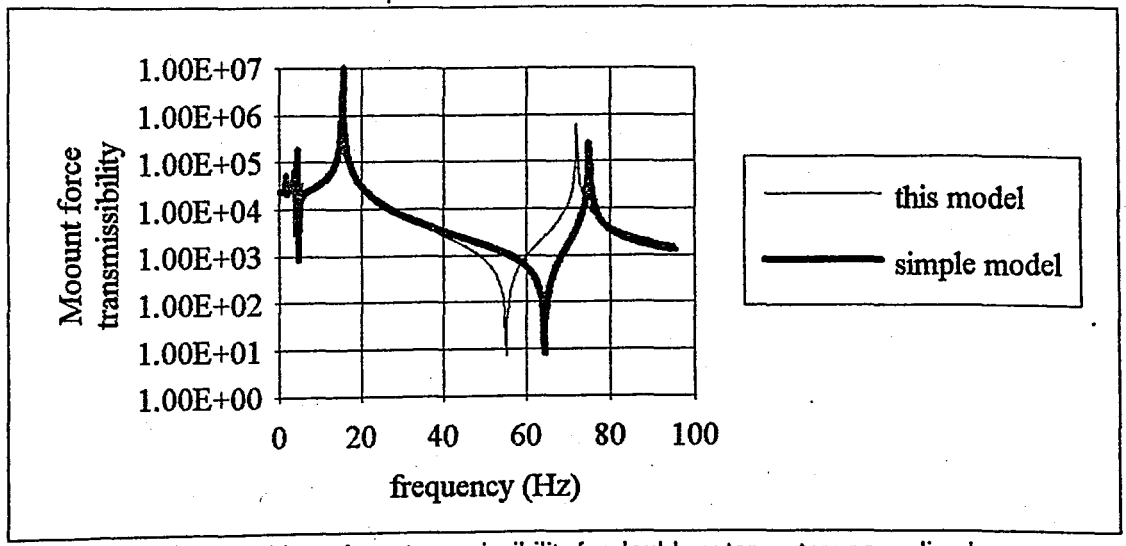

Fig. 4.16. Mount force transmissibility for double-rotor system normalized with respect to the unbalance force on the shaft.

5. CONCLUSIONS

A generic rotor bearing system model which is developed by Lim and Singh [1,12,13] has been employed. This system oriented model for precision rolling elemennt bearings includes rotating system, rolling element bearings, motor, rigid pedestals, rigid table and the flexible mount. The discrete shaft model includes torsional, flexural and longitudinal motions.

As a result of the experimental work it can be stated that dynamic analysis can well predict forced responses. Bearing and mount moment transmissibilities are predictable by this method, but conventional methods can not predict moment transmissibilities due to incomplete bearing stiffness matrix.

Some discrepancies of the experimental results from the theoretical ones are due to the followings:

(I) The dynamic analysis assumes the system undamped, but there is actually some damping in the system.

(II) The preload on the bearings is not predictable exactly, so some preload range is assumed.

(III) The effect of motor in vibration is not easy to predict.

(IV) Table is assumed to be rigid, but has some flexibility.

(V) Instruments used in measuring acceleration are not very sensitive. An example for the acceleration signal taken from first pedestal in single rotor system at 50 Hz is given in Fig. 5.1. Fast Fourier transform is made to this signal and the result is in Fig. 5.2. which shows that the signal has some noise.

The theory although restricted by the assumptions stated above and to a linear and time-invariant dynamic system, is comprehensive. It can be used for analysis as well as design studies of other rotating mechanical systems.

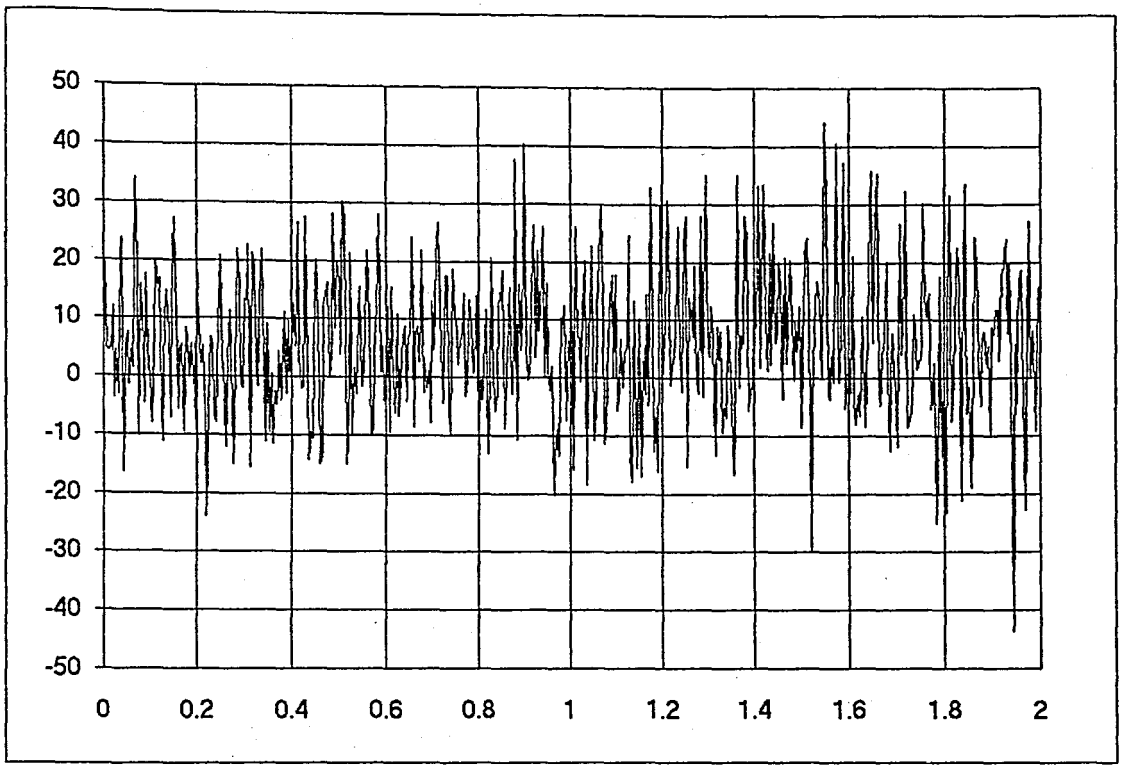

Fig. 5.1 Acceleration data acquiesced at 50 Hz from the pedestal located on the most left.

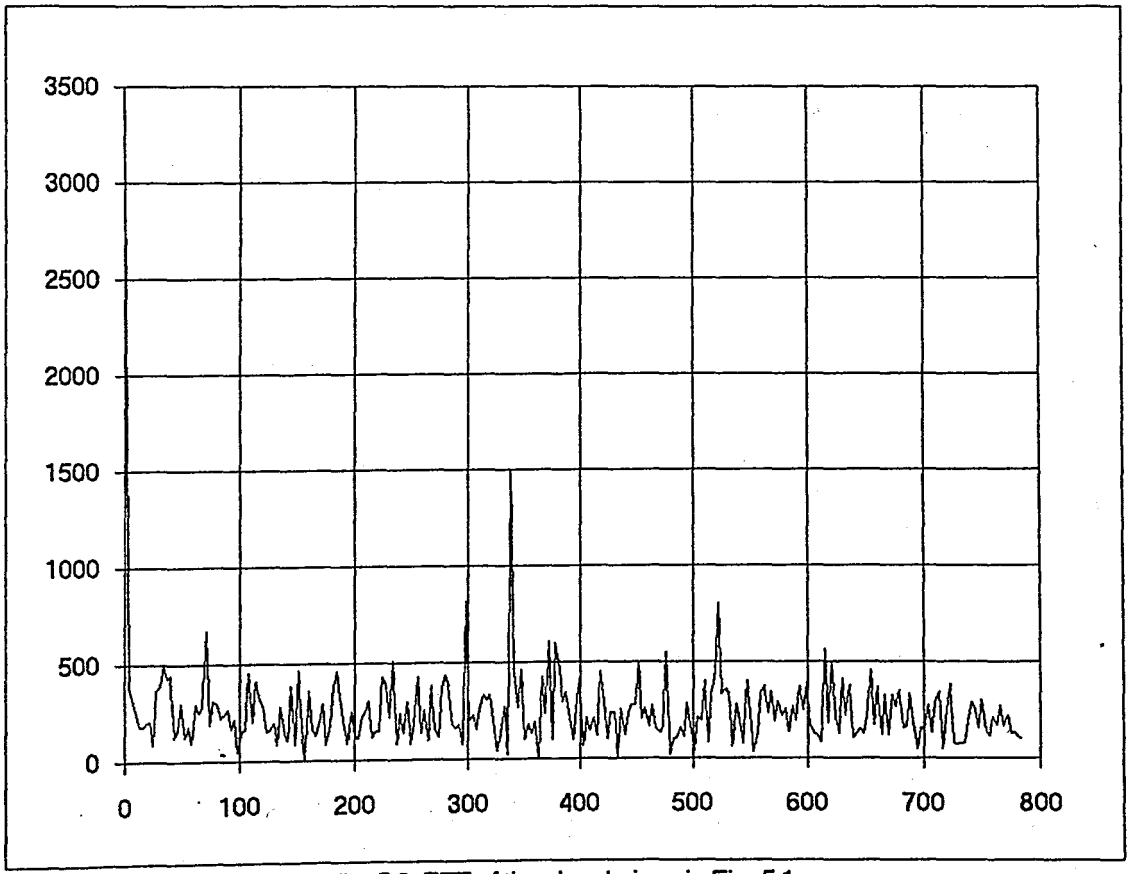

Fig. 5.2. FFT of the signal given in Fig. 5.1.

APPENDICES

APPENDIX 1

PROGRAM BEARING STIFFNESS

```
C     THIS PROGRAM CALCULATES EFFECTIVE BEARING STIFFNESSES ACCORDING
C     TO THE MEAN LOADS ON THE BEARING OR MEAN DISPLACEMENTS OF THE
C     BEARINGS. GIVEN DATA ARE ONLY FOR THE ANGULAR CONTACT TYPE OF
C     BEARINGS USED IN THE EXPERIMENTS. MEAN LOAD ON THE BEARING IS
C     AXIAL ONLY.
C     FORCE VECTOR ISAS [MX,MY,FX,FY,FZ]
C     DISPLACEMENT VECTOR IS AS [ΘX, ΘY, X,Y,Z]
C     STIFFNESSES ARE DEFINED SMILAR TO KBXX=D(3,3)


      DOUBLE PRECISION  X(5),F(5),Q(5),H(5),D(5,5),B(5,5),T(5)
      DOUBLE PRECISION DX(5),DT,ST,QT,G, FI(100),DZ(100),DR(100)
      DOUBLE PRECISION  DSZ(100),DSR(100),A(100),SINA(100),COSA(100)
      DOUBLE PRECISION AO,ANG,PI,RL,RJ,KN,ALO,N,KRR
      INTEGER BN,S,ITER
C     FORCES ARE ¯N (N), STIFFNESSES IN (N/M)
      PI=2*DACOS(0.D0)
      ITER=0
      N=1.5D0
      KN=1.7D6*(1000**1.5D0)
      RL=.00002D-3
      RJ=25.5D-3
      AO=.4366D-3
      ALO=40*PI/180.0D0
300   BN=11
      DO 5 I=1,5
 5    F(I)=0
      F(5)=10
      DO 7 I=1,5
 7    X(I)=0.D0
      X(5)=.025D-3
      WRITE(*,*)'FIRST GUESS OF DISP.VECTOR(BX,BY,X,Y,Z):'
      DO 8 I=1,5
 8    WRITE(*,*)X(I)
      ANG=2.0D0*PI/BN
      FI(1)=0
      DO 10 J=2,BN
 10   FI(J)=FI(J-1)+ANG
 1    FORMAT(4F8.4)
      CALL AJ(ALO,X,FI,DZ,DR,DSZ,DSR,A,SINA,COSA,
     C RJ,RL,AO,BN)
      ALL HJ(F,Q,KN,RJ,N,G,A,QT,BN,AO,SINA,COSA,FI,H)
```

```
11   CALL DERIVATIVE (PI,ALO,KRR,D,AO,KN,RJ,N,G,BN,DT
  C  ,FI,DSR,DSZ,A,DR,DZ)
     CALL GAUSSELIM (X,D,B,T,H,DX,S)
     DO 157 J=1,5
157  X(J)=X(J)+DX(J)
     CALL AJ(ALO,X,FI,DZ,DR,DSZ,DSR,A,SINA,COSA,
  C  RJ,RL,AO,BN)
     CALL HJ(F,Q,KN,RJ,N,G,A,QT,BN,AO,SINA,COSA,FI,H)
     CALL DERIVATIVE (PI,ALO,KRR,D,AO,KN,RJ,N,G,BN,DT
  C  ,FI,DSR,DSZ,A,DR,DZ)
     DO 158 J=1,5
     IF (ABS(H(J)).GT.(1D-5)) THEN
          ITER=ITER+1
          WRITE(*,*)'NEW ITERATION',ITER
          IF(ITER.EQ.100)STOP
          GO TO 170
     ENDIF
158  CONTINUE
     GO TO 180
170  WRITE(*,*) 'X(J),H(J),DX(J):'
     DO 159 J=1,5
159  WRITE (*,*) X(J),H(J),DX(J)
     GOTO 11
180  WRITE(*,*)'X(I),H(I):'
     DO 190 I=1,5
190  WRITE(*,*)'LV OF H(J):',H(I)
     STOP
     END



     SUBROUTINE AJ(ALO,X,FI,DZ,DR,DSZ,DSR,A,SINA,COSA,
   C  RJ,RL,AO,BN)
     DOUBLE PRECISION X(5),DZ(100),DR(100),DSZ(100)
     DOUBLE PRECISION FI(100),SINA(100),COSA(100)
     DOUBLE PRECISION DSR(100),A(100)
     DOUBLE PRECISION RJ,AO,RL,ALO
     INTEGER BN
     DO 20 J=1,BN
     DZ(J)=X(5)+RJ*(X(1)*SIN (FI(J))-X(2)*COS (FI(J)))
     DR(J)=X(3)*COS (FI(J))+X(4)*SIN (FI(J))-RL
     DSZ(J)=AO*SIN(ALO)+DZ(J)
     DSR(J)=AO*COS(ALO)+DR(J)
     A(J)=(DSZ(J)**2+DSR(J)**2)**.5
     SINA(J)=DSZ(J)/A(J)
     COSA(J)=DSR(J)/A(J)
20   CONTINUE
     RETURN
     END
```

```
      SUBROUTINE HJ(F,Q,KN,RJ,N,G,A,QT,BN,AO
     C ,SINA,COSA,FI,H)
      DOUBLE PRECISION F(5),Q(5),SINA(100),COSA(100)
      DOUBLE PRECISION FI(100),H(5),A(100),G,QT
      INTEGER BN
      DOUBLE PRECISION N,KN,RJ,AO,SIFI(100),COFI(100)
      DO 21 J=1,5
21    Q(J)=0
      DO 25 J=1,BN
      G=(A(J)-AO)
C     WRITE(*,*) SINA(J)
      IF (G.LT.0)  G=0
C     WRITE(*,*)'A(J)-AO=',G
      QT=KN*(G**N) * SINA(J)*RJ*SIN (FI(J))
      Q(1)=Q(1)+QT
      QT=-KN*(G**N) * SINA(J)*RJ*COS (FI(J))
      Q(2)=Q(2)+QT
      QT=KN*(G**N) * COSA(J)* COS (FI(J))
      Q(3)=Q(3)+QT
      QT=KN*(G**N) * COSA(J)*SIN (FI(J))
      Q(4)=Q(4)+QT
      QT=KN*(G**N) *SINA(J)
      Q(5)=Q(5)+QT
25    CONTINUE
      DO 30 J=1,5
30    H(J)=Q(J)-F(J)
      RETURN
      END



      SUBROUTINE DERIVATIVE(PI,ALO,KRR,D,AO,KN,RJ,N,G,BN
     C ,DT,FI,DSR,DSZ,A,DR,DZ)
      DOUBLE PRECISION D(5,5),FI(100),DSR(100),DSZ(100),A(100)
      DOUBLE PRECISION DT,G,KRR,SIFI(100),COFI(100)
      INTEGER BN
      DOUBLE PRECISION N,RJ,AO,KN,PI,ALO,DR(100),DZ(100)
      DO 31 I=1,5
      DO 31 J=1,5
31    D(I,J)=0
      KRR=0
      DO 33 J=1,BN
      G=A(J)-AO
      IF (G.LT.0) G=0
      DT=(KN*RJ*(G**N)*DSR(J)*DSZ(J)*SIN (FI(J))
     C *COS (FI(J))*((N*A(J)/(A(J)-AO)) -1))/A(J)**3
      D(1,3)=D(1,3)+DT
      D(3,1)=D(1,3)
      DT=KN*RJ*(G**N)*DSR(J)*DSZ(J)*((COS(FI(J)))**2)*
     C (1-(N*A(J)/(A(J)-AO)))/A(J)**3
      D(2,3)=D(2,3)+DT
      D(3,2)=D(2,3)
```

```
      DT=KN*RJ*(G**N)*DSR(J)*DSZ(J)*((SIN(FI(J)))**2)
     C *((N*A(J)/(A(J)-AO))-1)/A(J)**3
      D(1,4)=D(1,4)+DT
      D(4,1)=D(1,4)
      DT=KN*RJ*(G**N)*SIN(FI(J))*((N*A(J)*(DSZ(J)**2)
     C /(A(J)-AO))+A(J)**2-DSZ(J)**2)/A(J)**3
      D(1,5)=D(1,5)+DT
      D(5,1)=D(1,5)
      DT=KN*RJ*(G**N)*DSR(J)*DSZ(J)*SIN(FI(J))*COS(FI(J))
     C *(1-(N*A(J)/(A(J)-AO)))/A(J)**3
      D(2,4)=D(2,4)+DT
      D(4,2)=D(2,4)
      DT=KN*RJ*(G**N)*COS(FI(J))*((DSZ(J)**2)-(N*A(J)*(DSZ(J)
     C **2)/(A(J)-AO))-A(J)**2)/A(J)**3
      D(2,5)=D(2,5)+DT
      D(5,2)=D(2,5)
      DT=KN*RJ**2*(G**N)*((SIN(FI(J)))**2)*((N*A(J)*(DSZ(J)
     C **2)/(A(J)-AO))+A(J)**2-(DSZ(J)**2))/A(J)**3
      D(1,1)=D(1,1)+DT
      DT =KN*RJ**2*(G**N)*SIN(FI(J))*COS(FI(J))*
     C ((DSZ(J)**2)-(N*A(J)*DSZ(J)**2/(A(J)-AO))-A(J)**2)
      D(1,2)=D(1,2)+DT
      D(2,1)=D(1,2)
      DT=KN*RJ**2*(G**N)*((COS(FI(J)))**2)*((N*A(J)*
     C (DSZ(J)**2)/(A(J)-AO))+A(J)**2-(DSZ(J)**2))/A(J)**3
      D(2,2)=D(2,2)+DT
      DT=KN*(G**N)*((COS(FI(J)))**2)*((N*A(J)*(DSR(J)**2)
     C /(A(J)-AO))+A(J)**2-DSR(J)**2)/A(J)**3
      D(3,3)=D(3,3)+DT
      DT=KN*(G**N)*((N*A(J)*(DSR(J)**2))/(A(J)-AO)
     C +A(J)**2-DSR(J)**2)/A(J)**3
      KRR=KRR+DT
      DT=KN*(G**N)*SIN(FI(J))*COS(FI(J))*((N*A(J)*(DSR(J)**2)
     C /(A(J)-AO)) +A(J)**2-DSR(J)**2)/A(J)**3
      D(3,4)=D(3,4)+DT
      D(4,3)=D(3,4)
      DT=KN*(G**N)*(SIN(FI(J)))**2*((N*A(J)*(DSR(J)**2)/(A(J)-AO)
     C )+A(J)**2-DSR(J)**2)/A(J)**3
      D(4,4)=D(4,4)+DT
      DT=KN*(G**N)*DSR(J)*DSZ(J)*COS(FI(J))
     C *((N*A(J)/(A(J)-AO))-1)/A(J)**3
      D(3,5)=D(3,5)+DT
      D(5,3)=D(5,3)
      DT=KN*(G**N)*DSR(J)*DSZ(J)*SIN(FI(J))*((N*A(J)
     C /(A(J)-AO))-1)/A(J)**3
      D(4,5)=D(4,5)+DT
      D(5,4)=D(4,5)
      DT=KN*(G**N)*(N*A(J)*DSZ(J)**2/(A(J)-AO)+A(J)**2
     C -DSZ(J)**2)/A(J)**3
      D(5,5)=D(5,5)+DT
   33 CONTINUE
      RETURN
      END
```

```
      SUBROUTINE GAUSSELIM (X,D,B,T,H,DX,S)
      DOUBLE PRECISION X(5),D(5,5),B(5,5),T(5),H(5),DX(5)
      INTEGER S
      DO 501 J=1,5
501   H(J)=-H(J)
      DO 300 K=1,4
      IF (D(K,K) .EQ.0) THEN
           DO 34 I=K+1,5
           IF (D(I,K) .EQ. 0) GO TO 34
           S=I
          GO TO 101
34         CONTINUE
101        DO 150 I=K,5
150        B(K,I)=D(K,I)
           T(K)=H(K)
           H(K)=H(S)
           H(S)=T(K)
           DO 201 J=K,5
           D(K,J)=D(S,J)
           D(S,J)=B(K,J)
201        CONTINUE
      ENDIF
      L=K+1
      DO 220 I=L,5
      H(I)=H(I)-D(I,K)*H(K)/D(K,K)
      DO 220 J=L,5
      D(I,J)=D(I,J)-D(I,K)*D(K,J)/D(K,K)
220   CONTINUE
      DO 280 J=K+1,5
280   D(J,K)=0
300   CONTINUE
      DX(5)=H(5)/D(5,5)
      DX(4)=(H(4)-DX(5)*D(4,5))/D(4,4)
      DX(3)=(H(3)-DX(4)*D(3,4)-DX(5)*D(3,5))/D(3,3)
      DX(2)=(H(2)-DX(3)*D(2,3)-DX(4)*D(2,4)-DX(5)*D(2,5))/D(2,2)
      DX(1)=(H(1)-DX(2)*D(1,2)-DX(3)*D(1,3)-DX(4)*D(1,4)
     C  -DX(5)*D(1,5)) /D(1,1)
      DO 601 J=1,5
601   H(J)= -H(J)
      RETURN
      END
```

PROGRAM MATRIX PRODUCT

```
C     THIS PROGRAM CONSTRUCTS THE NEW FORM OF THE STIFFNESS MATRIX
C     FOR  THE ANALYSIS OF SINGLE-ROTOR SYSTEM AFTER MASS MOMENT OF
C     INERTIAS OF SHAFT SEGMENTS ARE NEGLECTED. BEARING STIFFNESSES ARE
C     CALCULATED BY PROGRAM BEARING STIFFNESS AND DENOTED BY 'KB---'.

      DOUBLE PRECISION A(17,17),B(17,17),P1(17,17),P(17,17),EI,LE
      DOUBLE PRECISION C(17,17),K12(9,9),S(17,17),K22(13,13),KB1XX
      DOUBLE PRECISION KB1XTY,KB1TYTY,KVX,KVTY,KB3TYTY,BI,PT(9,9)
      DOUBLE PRECISION KB2XX, KB2XTY, KB2TYTY, KB3XX, KB3XTY,
      DOUBLE PRECISION AAINVS(10,10),K23(5,5),K11(15,15),K13(15,13)AA(10,20)
      DOUBLE PRECISION KBTY,KBX
      INTEGER R,M
      OPEN(9,FILE='K1')
      OPEN(10,FILE='K2')
      OPEN(12,FILE='K4')
      KB1XX=4.5D+7
      KB1XTY=-9.68D5
      KB1TYTY=20732.5D0
      KB3XX=2.07D+8
      KB3XTY=-1.74D+5
      KB3TYTY=192.3D0
      KB2XX=KB1XX
      KB2XTY=KB1XTY
      KB2TYTY=KB1TYTY
      KVX=9D+4
      KVTY=(.93D0**2)*KVX
      WRITE(*,*)KVTY
      KBX=3*3.1415*(.01**2)*190D+9/(.06*4)
      KBTY=3*(190D+9*3.1415*(.005**4)/4)/.06
      EI=1.492D+3
      LE=.17D0
      Z1=-.287D0
      Z3=(.34D0-.287D0)
      Z4=(.515D0-.287D0)
      DO 5 I=1,3
      DO 5 J=1,3
5     AA(I,J)=0
      AA(1,1)=(4*EI/LE+KB1TYTY)
      AA(2,2)= (8*EI/LE+KB2TYTY)
      AA(2,3)=2*EI/LE
      AA(3,2)=2*EI/LE
      AA(3,3)=(4*EI/LE+KB3TYTY)
      N=3
      CALL INVT(AA,AAINVS,N)
      DO 10 I=1,N
      DO 10 J=1,N
10    A(I,J)=AAINVS(I,J)
1     FORMAT(F9.0)
      DO 45 K=1,8
      DO 45 L=1,8
      K11(K,L)=0
```

```
      K13(K,L)=0
45    CONTINUE
      K11(1,1)=12*EI/LE**3+KB1XX
      K11(1,2)=-12*EI/LE**3
      K11(1,5)= -KB1XX
      K11(2,1)=K11(1,2)
      K11(2,2)= -2*K11(1,2)
      K11(2,3)= K11(1,2)
      K11(3,1)= K11(1,3)
      K11(3,2)= K11(2,3)
      K11(3,3)=24*EI/LE**3+KB2XX
      K11(3,4)=-12*EI/LE**3
      K11(3,6)= -KB2XX
      K11(4,1)= K11(1,4)
      K11(4,2)= K11(2,4)
      K11(4,3)=K11(3,4)
      K11(4,4)=12*EI/LE**3+KB3XX
      K11(4,7)=-KB3XX
      K11(5,1)=-KB1XX
      K11(5,5)=KB1XX+KBX
      K11(5,8)=-KBX
      K11(6,3)=-KB2XX
      K11(6,6)=KB2XX+KBX
      K11(6,8)=-KBX
      K11(7,4)=-KB3XX
      K11(7,7)=KB3XX+KBX
      K11(7,8)=-KBX
      K11(8,5)=-KBX
      K11(8,6)=-KBX
      K11(8,7)=-KBX
      K11(8,8)=KBX*3+KVX
      DO 60 I=1,8
      DO 60 J=1,5
60    K12(I,J)=0
      K12(1,2)=-KB1XTY
      K12(1,1)=-6*EI/LE**2
      K12(3,1)= -K12(1,1)
      K12(3,3)=-KB2XTY
      K12(4,4)=-KB3XTY
      K12(5,2)=KB1XTY
      K12(5,5)=-Z1*KBX
      K12(6,3)=KB2XTY
      K12(6,5)=-Z3*KBX
      K12(7,4)=KB3XTY
      K12(7,5)=-Z4*KBX
      K12(8,5)=(Z1+Z3+Z4)*KBX
      K13(1,1)=-6*EI/LE**2+KB1XTY
      K13(2,1)= 6*EI/LE**2
      K13(2,2)= -K13(2,1)
      K13(3,2)=KB2XTY
      K13(3,3)=-6*EI/LE**2
      K13(4,2)=6*EI/LE**2
      K13(4,3)=6*EI/LE**2+KB3XTY
```

```
      K13(5,1)= -KB1XTY
      K13(6,2)= -KB2XTY
      K13(7,3)=-KB3XTY
      DO 70 I=1,5
      DO 70 J=1,5
70    K23(I,J)=0
      K23(1,1)=2*EI/LE
      K23(1,2)= 2*EI/LE
      K23(2,1)=-KB1TYTY
      K23(3,2)=-KB2TYTY
      K23(4,3)=-KB3TYTY
      DO 80 I=1,5
      DO 80 J=1,5
80     K22(I,J)=0
      K22(1,1)=8*EI/LE
      K22(2,2)= KB1TYTY+KBTY
      K22(2,5)=-KBTY
      K22(3,3)=KB2TYTY+KBTY
      K22(3,5)=-KBTY
      K22(4,4)=KB3TYTY+KBTY
      K22(4,5)=-KBTY
      K22(5,2)=-KBTY
      K22(5,3)=-KBTY
      K22(5,4)=-KBTY
      K22(5,5)=3*KBTY+KVTY+(Z1**2+Z3**2+Z4**2)*KBX
      DO 90 I=1,8
      DO 90 J=1,3
      B(J,I)=K13(I,J)
      P1(J,I)=0
90    CONTINUE
      DO 100 K=1,3
      DO 100 L=1,8
      DO 100 J=1,3
      P1(K,L)=P1(K,L)+A(K,J)*B(J,L)
100   CONTINUE
      DO 110 I=1,8
      DO 110J=1,3
      C(I,J)=K13(I,J)
 110  CONTINUE
      DO 120 I=1,8
      DO 120 J=1,8
      P(I,J)=0
120   CONTINUE
      DO 130 K=1,8
      DO 130 I=1,8
      DO 130 J=1,3
      P(K,I)=P(K,I)+C(K,J)*P1(J,I)
130     CONTINUE
2      FORMAT(D25.15)
      DO 135 J=1,8
      DO 135 L=1,8
      S(J,L)=K11(J,L)-P(J,L)
      WRITE(9,2)S(J,L)
```

```
135    CONTINUE
       DO140 I=1,5
       DO 140 J=1,3
       B(J,I)=K23(I,J)
       P1(J,I)=0
140 CONTINUE
       DO 150 K=1,3
       DO150 L=1,5
       DO150 J=1,3
       P1(K,L)=P1(K,L)+A(K,J)*B(J,L)
150 CONTINUE
       DO 160 I=1,8
       DO 160 J=1,5
       P(I,J)=0
160 CONTINUE
       DO 170 K=1,8
       DO 170 I=1,5
       DO 170 J=1,3
       P(K,I)=P(K,I)+C(K,J)*P1(J,I)
170 CONTINUE
       DO 175 J=1,8
       DO 175 L=1,5
       S(J,L)=K12(J,L)-P(J,L)
       WRITE(10,2)S(J,L)
175 CONTINUE
       DO 180 I=1,3
       DO 180 J=1,5
180 P1(I,J)=0
       DO 190 K=1,3
       DO 190 L=1,5
       DO 190 J=1,3
       P1(K,L)=P1(K,L)+A(K,J)*B(J,L)
190 CONTINUE
       DO 200 I=1,5
       DO 200 J=1,5
       P(I,J)=0
200 CONTINUE
       DO 210 I=1,5
       DO 210 J=1,3
       C(I,J)=K23(I,J)
210 CONTINUE
       DO 220 K=1,5
       DO 220 I=1,5
       DO 220 J=1,3
       P(K,I)=P(K,I)+C(K,J)*P1(J,I)
220 CONTINUE
       DO 230 J=1,5
       DO 230 L=1,5
       S(J,L)=K22(J,L)-P(J,L)
       WRITE(12,2)S(J,L)
230 CONTINUE
       STOP
       END
```

```
      SUBROUTINE INVT (AA,AAINVS,N)
      DOUBLE PRECISION A,B,D(10,20),AA(10,20),AAINVS(10,10)
     C ,QUOT,TEMP,UNIT(10,10)
      DATA UNIT /100*0.0/
      NT2=N*2
      NP1=N+1
      NM1=N-1
      DO 10 I=1,N
   10 UNIT(I,I)=1
      DO 11 I=1,N
      DO 11 J=1,N
      D(I,J)=AA(I,J)
   11 D(I,N+J)=UNIT(I,J)
      DO 42 J=1,NM1
      A=DABS(D(J,J))
      JP1=J+1
      DO 43 I=JP1,N
      B=DABS(D(I,J))
      IF (A-B) 20, 43, 43
   20 DO 44 K=J,NT+2
      TEMP=D(I,K)
      D(I,K)=D(J,K)
   44 D(J,K)=TEMP
   43 A=B
      DO 42 I=JP1,N
      QUOT=D(I,J)/D(J,J)
      DO 42 K=JP1,NT2
   42 D(I,K)=D(I,K)-QUOT*D(J,K)
      K=N
   15  I=K-1
   12 QUOT=D(I,K)/D(K,K)
      DO 45 J=NP1,NT2
   45 D(I,J)=D(I,J)-QUOT*D(K,J)
      IF(I.EQ.1) GO TO 13
      I=I-1
      GOTO 12
   13 IF (K.EQ.2) GO TO 14
      K=K-1
      GO TO 15
   14 DO 46 I=1,N
      DO 46 J=1,N
   46 AAINVS(I,J)=D(I,N+J)/D(I,I)
      RETURN
      END
```

PROGRAM JACOBI

```
C     THIS PROGRAM CALCULATES NATURAL FREQUENCY OF THE SINGLE-ROTOR
C     SYSTEM. BEFORE RUNNING THIS PROGRAM, MATRIX PRODUCT SHOULD
C     BE RUN. THE STIFFNESS MATRIX OF THE SYSTEM AFTER THE MASS
C     MOMENT INERTIAS OF SHAFT  SEGMENTS ARE NEGLECTED IS CONSTRUCTED
C     IN PROGRAM MATRIX PRODUCT

      DOUBLE PRECISION R(14,14),S(14,14),M(14,14),A(14,14),FT4
      DOUBLE PRECISION P(14,14),P1(14,14),RT(14,14),MOD(17,17)
      DOUBLE PRECISION PROD(17,17),SM(14,28),SMINVS(14,28),W
      DOUBLE PRECISION X(14),FL(14),Q,PT(14,14),XDD(14),FT1,MT1
      INTEGER T,F,E
      OPEN(9,FILE='K1')
      OPEN(10,FILE='K2')
      OPEN(12,FILE='K4')
      OPEN(26,FILE='AC5')
      OPEN(25,FILE='AC6')
      N=13
      DO 10 I=1,N
10    FL(I)=0
      DO 6 I=1,N
      DO 6 J=1,N
      MOD(I,J)=0
      M(I,J)=0
6     CONTINUE
      M(1,1)=SQRT(1.0D0/(1.35D0/6.D0))
      M(2,2)=SQRT(1.0D0/(1.3*2+1.35/3))
      M(3,3)=SQRT(1.0D0/(1.35/3))
      M(4,4)=SQRT(1.0D0/(1.35D0/6.D0))
      M(5,5)=SQRT(1/(8.5D0))
      M(6,6)=SQRT(1/(8.5D0))
      M(7,7)=SQRT(1/(8.5D0))
      M(8,8)=SQRT(1.D0/25.D0)
      M(9,9)=SQRT(1/(2*.89D-3))
      M(10,10)=SQRT(1/(8.5*(.045**2+.16**2)/12))
      M(11,11)=M(10,10)
      M(12,12)=M(10,10)
      M(13,13)=SQRT(1.D0/(10*.5**2+15*.25**2))
      DO 1 I=1,N
      DO 1 J=1,N
      IF (I.EQ.J) MOD(I,J)=M(J,I)
1     CONTINUE
99    FORMAT(F28.0)
      DO 103 I=1,8
      DO 108 J=1,8
      READ(9,99)S(I,J)
108   CONTINUE
      DO 104 J=9,13
      READ(10,99)S(I,J)
104   CONTINUE
103   CONTINUE
      CLOSE (9)
```

```
      CLOSE(10)
      DO 102 I=9,13
      DO 102 J=9,13
      READ(12,99)S(I,J)
102   CONTINUE
      CLOSE (12)
      OPEN(11,FILE='M')
      DO 105 I=1,N
      DO 105 J=1,N
105   S(J,I)=S(I,J)
      DO 8 I=1,N
      DO 8 J=1,N
      P1(I,J)=0
8     CONTINUE
      DO 27 I=1,N
      DO 28 L=1,N
      DO 22 J=1,N
      P1(I,L)=P1(I,L)+S(I,J)*M(J,L)
      P(I,L)=0
22    CONTINUE
28    CONTINUE
27    CONTINUE
      DO 30 I=1,N
      DO 30 L=1,N
      DO 30 J=1,N
      P(I,L)=P(I,L)+M(I,J)*P1(J,L)
30    CONTINUE
      IT=1
32    DO 300 I=1,N
      DO 35 T=1,N
      IF(T.EQ.I) GO TO 35
      Q=DATAN(2*P(I,T)/(P(I,I)-P(T,T)))/2
      DO 36 K=1,N
      DO 36 L=1,N
      R(K,L)=0.D0
      IF(K.EQ.L) R(K,L)=1
36    CONTINUE
      R(I,I)=DCOS(Q)
      R(I,T)=-DSIN(Q)
      R(T,I)=DSIN(Q)
      R(T,T)=DCOS(Q)
      DO 38 K=1,N
      DO 38 J=1,N
      RT(K,J)=R(J,K)
38    CONTINUE
      DO 39 K=1,N
      DO 39 J=1,N
      P1(K,J)=0
39    CONTINUE
      DO 40 K=1,N
      DO 40 L=1,N
      DO 40 J=1,N
      P1(K,L)=P1(K,L)+P(K,J)*R(J,L)
```

```
      A(K,L)=0
40    CONTINUE
      DO 50 K=1,N
      DO 50 L=1,N
      DO 50 J=1,N
      A(K,L)=A(K,L)+RT(K,J)*P1(J,L)
50    CONTINUE
      DO 100 K=1,N
      DO 100 L=1,N
      P(K,L)=A(K,L)
100   CONTINUE
      DO 800 K=1,N
      D0O 800 L=1,N
800   PROD(K,L)=0
      DO 801 K=1,N
      DO 801 L=1,N
      DO 801 E=1,N
801   PROD(K,L)=RT(K,E)*MOD(E,L)+PROD(K,L)
      DO 802 K=1,N
      DO 802 L=1,N
802   MOD(K,L)=PROD(K,L)
35    CONTINUE
300   CONTINUE
      DO 45 I=1,N
      DO 45 J=1,N
      IF(I.EQ.J) GO TO 45
      H=ABS(A(I,J))
      IF(A(I,J) .GT. H) THEN
      DO 46 F=1,N
      DO 46 L=1,N
      P(L,F)=A(L,F)
46    CONTINUE
      IT=IT+1
      GO TO 32
      ENDIF
45    CONTINUE
      DO 60 I=1,N
      DO 805 J=1,N
805   WRITE(11,*)'MOD(',J,I,')=',MOD(I,J)
      WRITE(11,*)'W(',I,I,')=',SQRT((A(I,I)))/(2*3.1415)
60    CONTINUE
      DO 939 W=1,600
      FL(4)=-.01*(W**2)*.135
      FL(8)=.015*(W**2)*.135
      FL(13)=FL(8)*(.35)
      FL(2)=.03*(W**2)*.06
      DO 832 I=1,N
      DO 832 J=1,N
      SM(I,J)=S(I,J)-M(I,J)*(W**2)
32    CONTINUE
      CALL INVT (SM,SMINVS,N)
      DO 903 I=1,N
      DO 903 J=1,N
```

```
903  PT(I,J)=0
     DO 902 K=1,N
     DO 902 L=1,N
     DO 902 I=1,N
902  PT(K,L)=PT(K,L)+SMINVS(K,I)*SM(I,L)
     DO 904 I=1,N
     DO 904 J=1,N
904  CONTINUE
     DO 834 K=1,N
834  X(K)=0
     DO 833 K=1,N
     DO 833 I=1,N
833  X(K)=X(K)+SMINVS(K,I)*FL(I)
     DO 837 K=1,N
     XDD(K)=-X(K)*(W**2)
837  CONTINUE
939  CONTINUE
     CLOSE (11)
     CLOSE (26)
     CLOSE (25)
     STOP
     END
```

APPENDIX 2

System stiffness matrix is

$$[K]=\begin{bmatrix} K_{11} & K_{12} & K_{13} \\ K_{21} & K_{22} & K_{23} \\ K_{31} & K_{32} & K_{33} \end{bmatrix}, K_{21}=K_{12}^{T}, K_{31}=K_{13}^{T}, K_{32}=K_{23}^{T}$$

where

$$K11=\begin{bmatrix}
12*EI/LE^3+KB1XX & -12*EI/LE^3 & 0 & 0 & -KB1XX & 0 & 0 & 0 \\
-12*EI/LE^3 & 24*EI/LE^3 & -12*EI/LE^3 & 0 & 0 & 0 & 0 & 0 \\
0 & -12*EI/LE^3 & 24*EI/LE^3+KB2XX & -12*EI/LE^3 & -KB2XX & 0 & 0 & 0 \\
0 & 0 & -12*EI/LE^3 & 12*EI/LE^3 +KB3XX & 0 & 0 & -KB3XX & 0 \\
-KB1XX & 0 & 0 & 0 & KB1XX+ KBX & 0 & 0 & -KBX \\
0 & 0 & -KB2XX & 0 & 0 & KB2XX+ KBX & 0 & -KBX \\
0 & 0 & 0 & -KB3XX & 0 & 0 & KB3XX+ KBX & -KBX \\
0 & 0 & 0 & 0 & -KBX & -KBX & -KBX & 3*KBX+ KVX
\end{bmatrix}$$

$$K12=\begin{bmatrix} -6*EI/LE^2 & -KB1X\theta_V & 0 & 0 & 0 \\ 0 & 0 & 0 & 0 & 0 \\ 6*EI/LE^2 & 0 & -KB2X\theta_V & 0 & 0 \\ 0 & 0 & 0 & -KB3X\theta_V & 0 \\ 0 & KB1X\theta_V & 0 & 0 & -Z1*KBX \\ 0 & & KB2X\theta_V & 0 & -Z3*KBX \\ 0 & 0 & 0 & KB3X\theta_V & -Z4*KBX \\ 0 & 0 & 0 & 0 & (Z1+Z3+Z4)*KBX \end{bmatrix}$$

$$K13=\begin{bmatrix} -6*EI/LE^2+KB1X\theta_V & 0 & 0 \\ 6*EI/LE^2 & -6*EI/LE^2 & 0 \\ 0 & KB2XTY & -6*EI/LE^2 \\ 0 & 6*EI/LE^2 & 6*EI/LE^2+KB3X\theta_V \\ -KB1XX\theta_V & 0 & 0 \\ 0 & -KB2XX\theta_V & 0 \\ 0 & 0 & -KB3XX\theta_V \\ 0 & 0 & 0 \end{bmatrix}$$

$$K22=\begin{bmatrix} 8*EI/LE & 0 & 0 & 0 & 0 \\ 0 & KB1\theta_V\theta_V+KB\theta_V & & 0 & -KB\theta_V \\ 0 & 0 & KB2\theta_V\theta_V+KB\theta_V & & -KB\theta_V \\ 0 & 0 & 0 & KB3\theta_V\theta_V+kb\theta_V & -KB\theta_V \\ 0 & -KB\theta_V & -KB\theta_V & -KB\theta_V & 3*KBTY+KVT\dot{Y}+(z1* \\ & & & & *KB1X\theta_V+Z3*KB2X\theta \\ & & & & {}_V+Z4*KB3X\theta_V)+(Z1^2 \\ & & & & *KB1XX+Z3^2*KB2X \\ & & & & X+Z4^2*KB3XX) \end{bmatrix}$$

$$K23=\begin{bmatrix} 2*EI/LE & 2*EI/LE & 0 \\ -KB1\theta_V\theta_V & 0 & 0 \\ 0 & -KB2\theta_V\theta_V & 0 \\ 0 & 0 & -KB3\theta_V\theta_V \\ 0 & 0 & 0 \end{bmatrix}$$

$$K33=\begin{bmatrix} (4*EI/LE+KB1\theta_V\theta_V) & 0 & 0 \\ 0 & (8*EI/LE+KB2\theta_V\theta_V) & 2*EI/LE \\ 0 & 2*EI/LE & (4*EI/LE+KB3\theta_V\theta_V) \end{bmatrix}$$

$$M = \begin{bmatrix} M_{s1} & & & & & & & & & & & & \\ & M_{s2}+M_R & & & & & & & & & & & \\ & & M_{s3} & & & & & & & & & & \\ & & & M_{s4} & & & & & & & & & \\ & & & & M_{n1} & & & & & & & & \\ & & & & & M_{n2} & & & & & & & \\ & & & & & & M_{n3} & & & & & & \\ & & & & & & & M_T & & & & & \\ & & & & & & & & I_{vR} & & & & \\ & & & & & & & & & I_{vn1} & & & \\ & & & & & & & & & & I_{vn2} & & \\ & & & & & & & & & & & I_{vn3} & \\ & & & & & & & & & & & & I_{vT} \end{bmatrix}$$

APPENDIX 3

Table App. 3.1
Natural frequencies (Hz.) of the single-rotor system for vibration in the y-direction.

1	6
2	20
3	87
4	96
5	97
6	108
7	123
8	148
9	196
10	868
11	1522
12	1609
13	4918

Corresponding modal matrix ,whose columns are the modal vectors;

$$\begin{bmatrix}
-0.14 & -0.15 & -0.10 & 0.16 & 0.00 & -0.17 & -0.27 & 0.10 & -0.22 & -0.2 & 2.03 & 0.19 & 0.00 \\
-0.14 & -0.08 & -0.28 & -0.04 & 0.00 & 0.25 & -0.03 & 0.11 & 0.38 & 0.01 & 0.03 & -0.03 & 0.00 \\
-0.14 & 0.01 & -0.18 & -0.11 & 0.00 & 0.18 & 0.14 & 0.02 & -0.17 & -0.3 & -0.16 & 1.40 & 0.00 \\
-0.14 & 0.11 & 0.03 & -0.04 & -0.02 & -0.17 & 0.11 & 0.19 & 0.05 & 0.00 & 0.00 & 0.00 & 2.08 \\
-0.14 & -0.13 & 0.03 & -0.02 & 0.02 & -0.02 & -0.24 & 0.11 & -0.09 & -0.01 & -0.06 & -0.01 & 0.00 \\
-0.14 & 0.03 & -0.02 & 0.06 & 0.00 & 0.19 & 0.13 & 0.05 & -0.18 & 0.03 & 0.01 & -0.06 & 0.00 \\
-0.14 & 0.11 & 0.03 & -0.04 & -0.01 & -0.17 & 0.10 & 0.19 & 0.05 & 0.00 & 0.00 & 0.00 & -0.05 \\
-0.14 & 0.01 & 0.03 & 0.00 & 0.00 & -0.03 & 0.00 & -0.14 & 0.03 & 0.00 & 0.00 & 0.00 & 0.00 \\
0.00 & -0.47 & 0.31 & 0.87 & 0.01 & -1.21 & -1.34 & 0.40 & 0.41 & 22.8 & 1.34 & 5.91 & -0.07 \\
0.00 & 0.54 & 6.88 & -6.85 & 0.68 & 4.25 & 0.04 & 0.58 & 1.38 & 0.25 & 1.38 & 0.16 & 0.00 \\
0.01 & 0.45 & 5.77 & 7.89 & 0.08 & 2.01 & -0.76 & 1.81 & 3.38 & -0.74 & -0.16 & 1.34 & 0.02 \\
0.00 & 0.46 & -0.49 & 0.37 & 10.8 & -0.39 & 0.47 & 0.01 & -0.03 & 0.00 & 0.00 & 0.00 & 0.05 \\
0.00 & 0.45 & -0.07 & 0.00 & -0.01 & 0.08 & -0.27 & -0.03 & -0.03 & 0.00 & 0.00 & 0.00 & 0.00
\end{bmatrix}$$

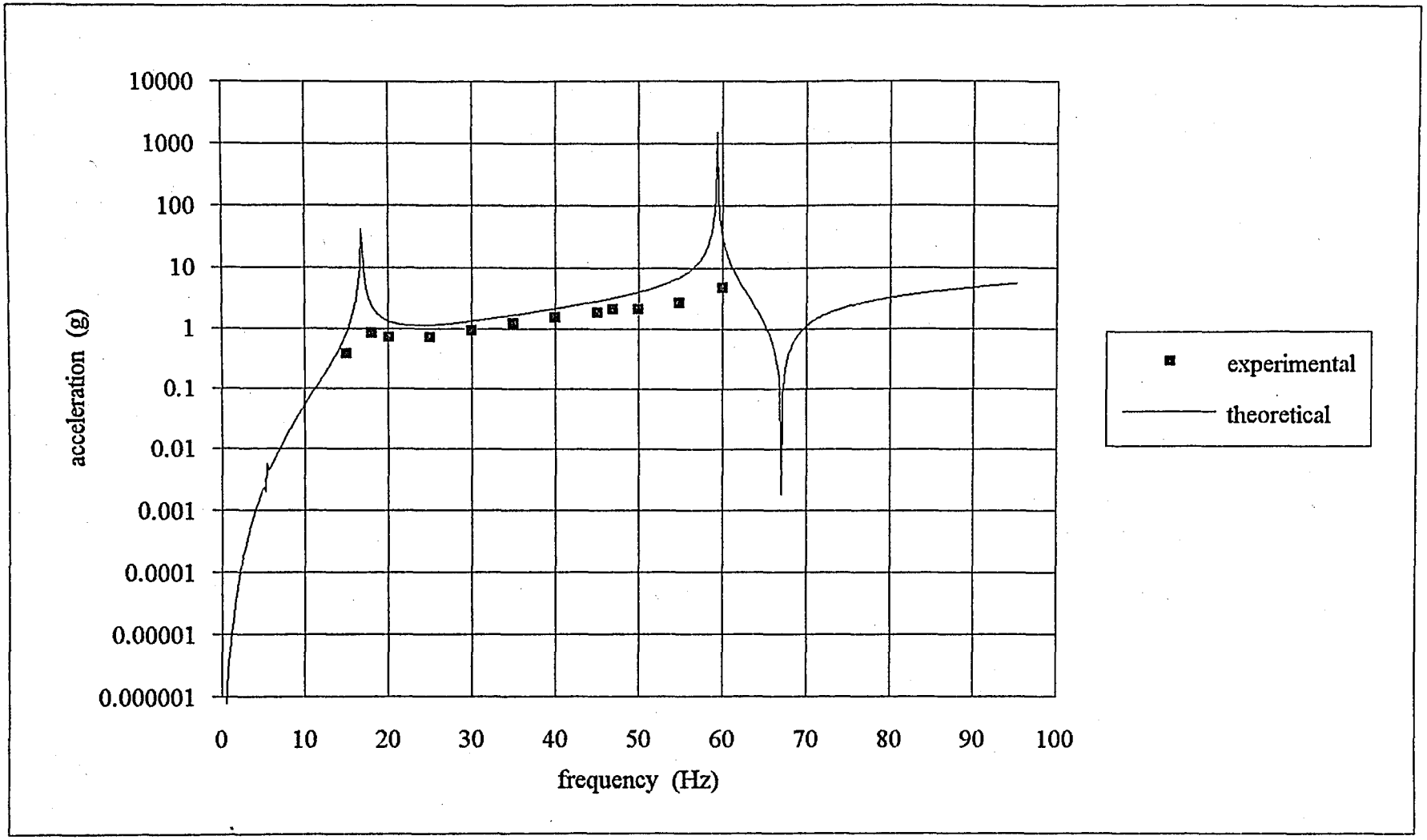

Figure App3.1. Comparison of experimental and theoretical results in y-direction for pedestal 1 in single rotor system . Accelerations are normalized with respect to g.

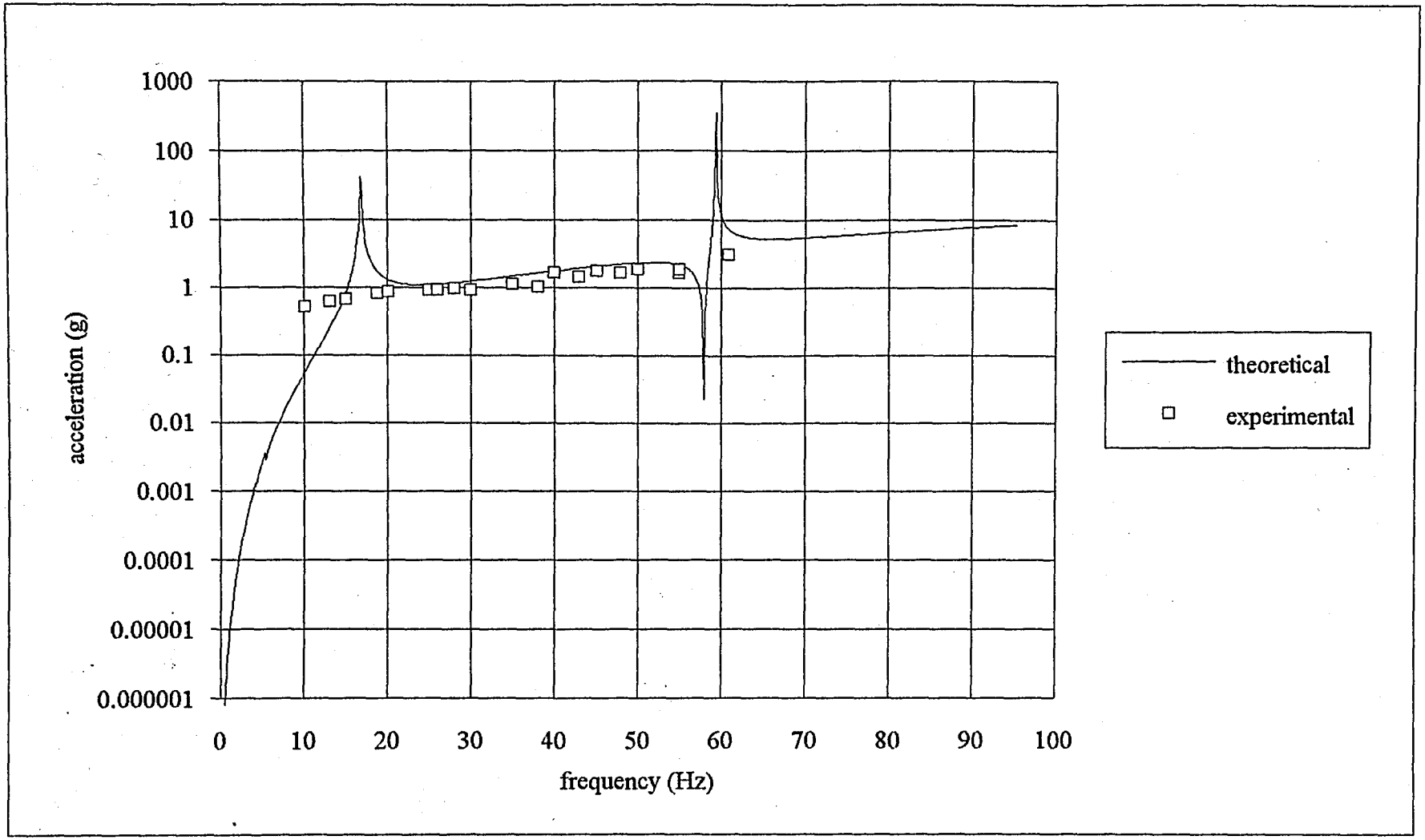

Figure App3.2. Comparison of experimental and theoretical results in y-direction of pedestal 2 in single rotor system. Accelerations are normalized with respect to g.

Table App. 3.2
Natural frequencies of the double rotor-system
for vibration in the y-direction

1	6.303
2	22.5
3	90.01
4	109.9
5	127.5
6	146.2
7	170.9
8	299.6
9	347.4
10	561.4
11	1316
12	1732
13	1795
14	2263
15	5694

Corresponding modal matrix whose columns are the modal vectors,

$$\begin{bmatrix}
0.14 & -0.17 & -0.15 & -0.20 & -0.24 & -0.04 & 0.22 & 0.00 & 0.16 & 0.14 & -0.03 & 2.03 & 1.25 & -0.02 & 0.00 \\
0.14 & -0.12 & -0.24 & 0.23 & -0.12 & -0.14 & -0.22 & 0.00 & -0.42 & -0.44 & -0.11 & -0.01 & 0.10 & -0.03 & 0.00 \\
0.14 & -0.06 & -0.22 & 0.41 & 0.02 & -0.14 & -0.31 & 0.00 & 0.08 & 0.48 & -0.01 & 0.08 & -0.12 & -0.05 & 0.00 \\
0.14 & 0.02 & -0.10 & 0.23 & 0.10 & -0.10 & -0.08 & -0.01 & 0.53 & -0.14 & -0.41 & -0.27 & 0.45 & 1.45 & -0.02 \\
0.14 & 0.12 & 0.04 & -0.13 & 0.08 & -0.23 & -0.02 & -0.03 & -0.02 & 0.01 & 0.01 & 0.00 & 0.00 & 0.02 & 2.41 \\
0.14 & -0.15 & 0.04 & -0.02 & -0.23 & -0.07 & 0.11 & 0.00 & 0.04 & 0.03 & 0.02 & -0.05 & -0.02 & 0.00 & 0.00 \\
0.14 & 0.04 & -0.05 & 0.15 & 0.14 & 0.02 & 0.22 & 0.00 & 0.04 & -0.06 & 0.03 & 0.01 & -0.02 & -0.04 & 0.00 \\
0.14 & 0.12 & 0.04 & -0.13 & 0.08 & -0.24 & -0.03 & 0.00 & -0.04 & 0.02 & 0.00 & 0.00 & 0.00 & 0.00 & -0.05 \\
0.14 & 0.01 & 0.02 & -0.04 & 0.01 & 0.12 & -0.07 & 0.00 & 0.00 & 0.00 & 0.00 & 0.00 & 0.00 & 0.00 & 0.00 \\
0.00 & -0.47 & 0.41 & -2.86 & -1.14 & 0.47 & 2.57 & -0.02 & 0.59 & -3.77 & -20.32 & 12.94 & -22.30 & 3.84 & 0.00 \\
0.00 & -0.57 & -0.64 & 0.10 & -1.04 & -0.39 & -1.04 & 0.08 & -6.42 & -2.80 & 24.02 & 9.54 & -13.59 & 14.80 & -0.22 \\
0.00 & 0.64 & 9.35 & 4.97 & -0.24 & -0.77 & -1.13 & 0.01 & -0.91 & -0.67 & -0.35 & 1.15 & 0.46 & 0.01 & 0.00 \\
0.00 & 0.34 & 1.01 & -1.02 & 1.09 & 5.33 & 11.03 & 0.66 & -24.21 & 16.08 & -6.04 & -2.38 & 3.67 & 8.31 & 0.15 \\
0.00 & 0.49 & -0.11 & 0.12 & -0.46 & 0.03 & -0.11 & 33.50 & 0.70 & -0.21 & 0.03 & 0.01 & -0.01 & 0.01 & 0.38 \\
0.00 & 0.50 & -0.08 & 0.09 & -0.35 & 0.07 & 0.03 & -0.01 & 0.01 & 0.00 & 0.00 & 0.00 & 0.00 & 0.00 & 0.00
\end{bmatrix}$$

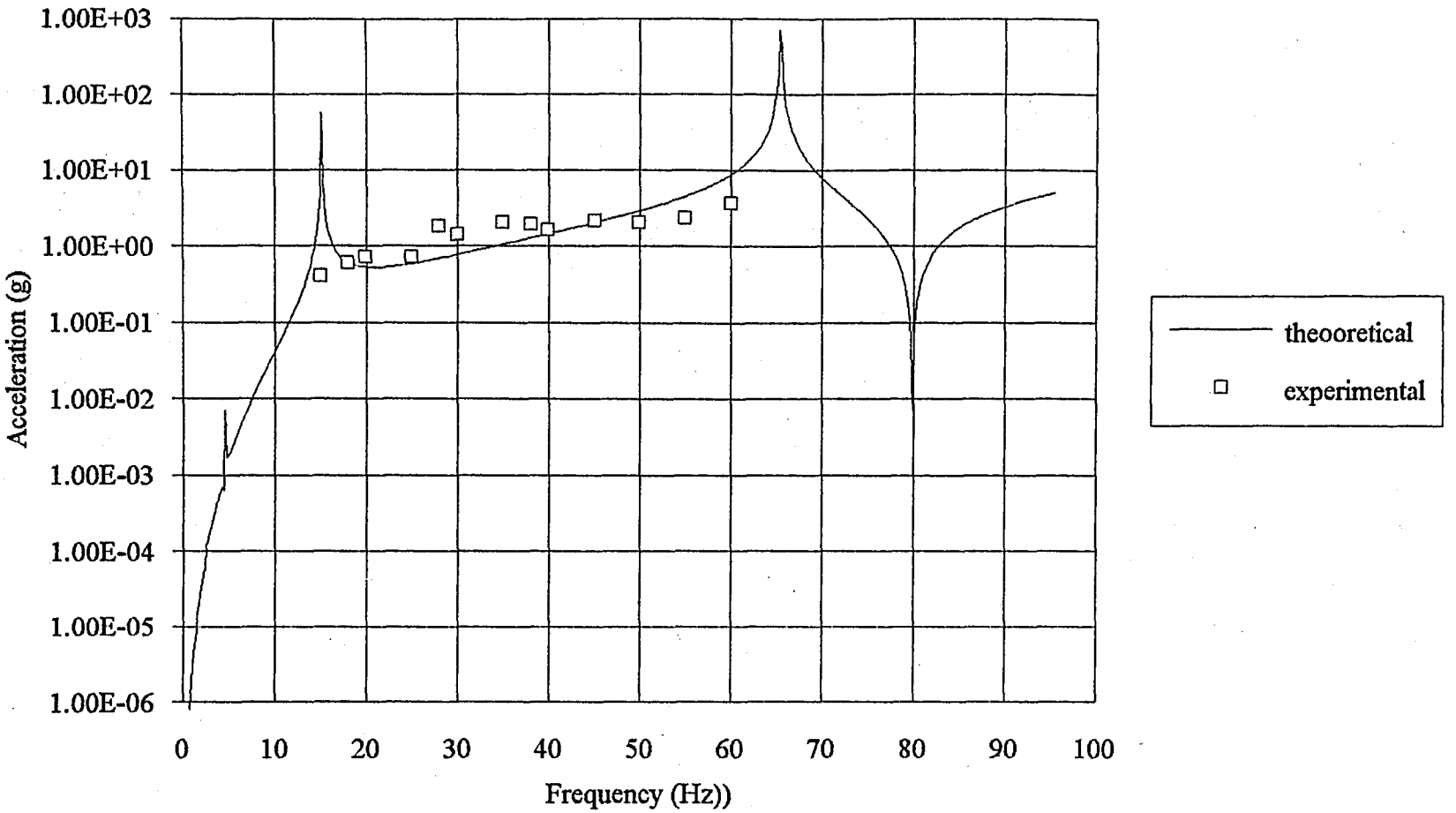

Figure App.3.3. Comparison of experimentaland theoretical results in y-direction of pedestal 1 in double rotor system. Accelerations are normalized with respect to g.

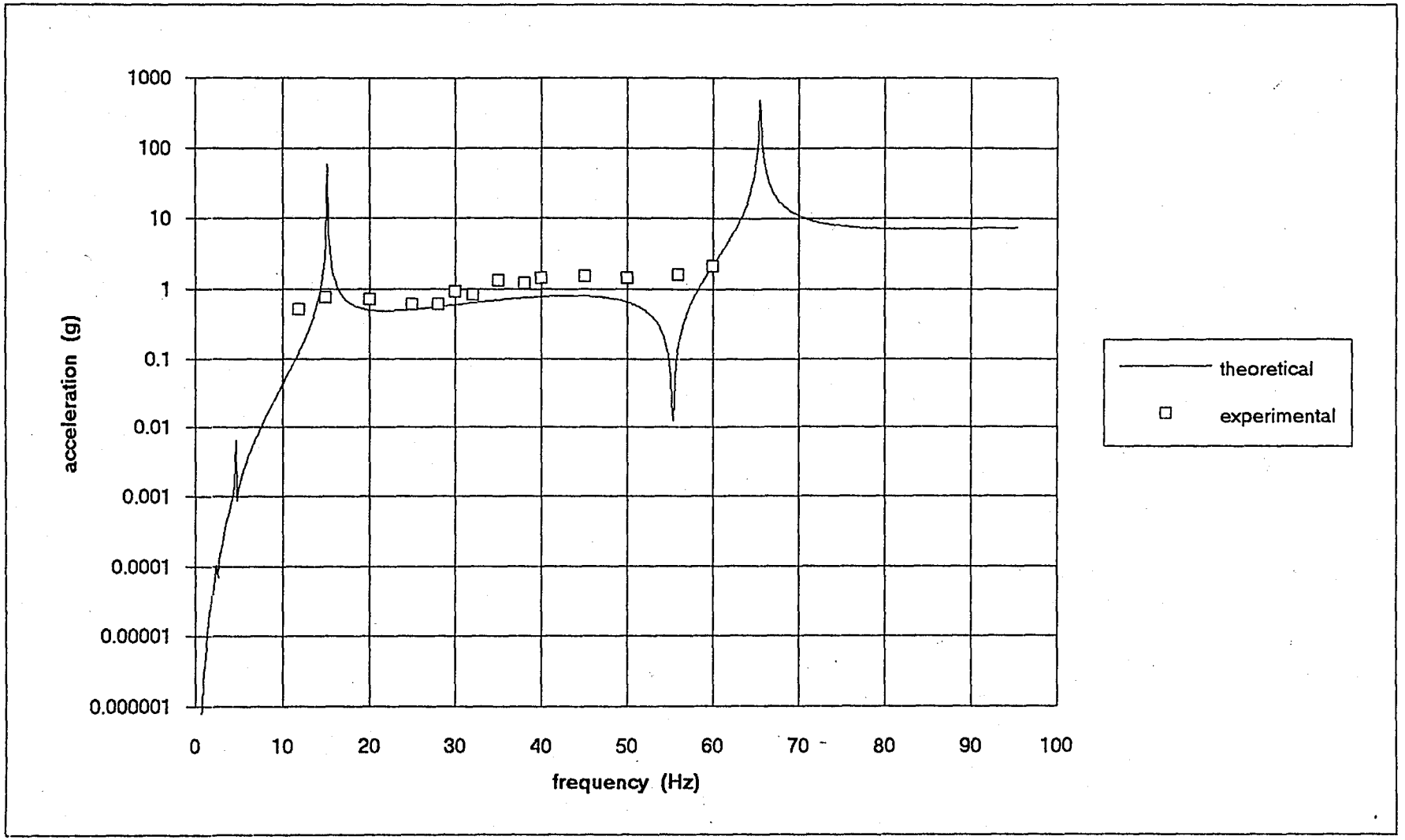

Figure App.3.4. Comparison of theoretical and experimental results in the y-direction of pedestal 2 in double-rotor system. Accelerations are normalized with respect to g.

REFERENCES

1. LIM, T. C. , "Vibration Transmission Through Rolling Element Bearings, Part I: Bearing Stiffness Formulation," Journal of Sound and Vibration, Vol. 139, pp. 179-199, 1990.

2. ÖZGÜVEN, H. N., "On the Critical Speed of Continuous Shaft-Disk Systems," Journal of Vibration, Acoustics, Stress, and Reliability in Design, Vol. 106, pp.59-61, 1984.

3. ZORZI, E. S., NELSON, H. D., "Finite Element Simulation of Rotor-Bearing Systems With Internal Damping," Journal of Engineering for Power, pp. 71-76, January, 1977.

4. HARRIS, T. A., Rolling Bearing Analysis, John Wiley, New York, 1966.

5. GARGIULO, E.P., "A Simple way to estimate bearing stiffness," Machine Design, Vol. 52, pp.107-110, 1980.

6. WHILE, M. F., "Rolling Element Bearing Vibration Transfer Characteristics: Effect of Stiffness," Journal of Applied Mechanics, Vol. 46, pp. 677-684, 1979.

7. WALFORD, T. L. H., STONE, B. J.," The measurement of the radial stiffness of rolling element bearings under oscillation conditions," Journal of Mechanical Engineering Science, Vol. 22, pp.175-181, 1980.

8. KRAUS, J., BLECH, J. J., BRAUN, S. G., "In Situ Determination of Rolling Bearing Stiffness and Damping by Modal Analysis," Journal of Vibration, Acoustics, Stress, and Reliability in Design, Vol. 109, pp. 235-240, 1987.

9. LIM, T. C. , "Vibration Transmission Through Rolling Element Bearings, Part III: Geared Rotor System Studies," Journal of Sound and Vibration, Vol. 151, pp. 31-54, 1991.

10. LIM, T. C. , "Vibration Transmission Through Rolling Element Bearings, Part II: System Studies," Journal of Sound and Vibration, Vol. 139, pp. 201-225, 1990.

11. HOUGHTON, P. S., Ball and Roller Bearings, Applied Science Publishers Ltd, London, 1976.

UNCITED REFERENCES

1. LIM, T. C. , "Vibration Transmission Through Rolling Element Bearings, Part IV: Statistical Energy Analysis," Journal of Sound and Vibration, Vol. 153, pp. 37-50, 1992.

2. LIM, T. C. , "Force and Moment Transmissibilities Through Rolling Element Bearing in a Single-stage Rotor System,"Proceedings of the 8th Internationam Modal Analysis Conference, Kissimmee, Florida pp. 704-710, 1989.

3. KAHRAMAN, A., SINGH, R., "Non-linear Dynamics of a Geared Rotor-bearing Systemwith Multiple Clearances," Journal of Sound and Vibration, Vol. 144, pp. 469-506, 1991.

4. LUND, J. W., WANG, Z., "Application of the Riccati Method to Rotor Dynamic Analysis of Long shafts on a Flexible foundation," Journal of Vibration, Acoustics, Stress, and Reliability in Design, Vol. 108, pp.177-181, 1986.

5. MEIROVITCH, L., "Computational Methods in Structural Dynamics," Sijthoff & Noordhoff, U.S.A., 1980